Advances in Intelligent Systems and Computing 267

Roman Szewczyk
Cezary Zieliński
Małgorzata Kaliczyńska *Editors*

Recent Advances in Automation, Robotics and Measuring Techniques

Springer

Advances in Intelligent Systems and Computing

Volume 267

Series editor

Janusz Kacprzyk, Polish Academy of Sciences, Warsaw, Poland
e-mail: kacprzyk@ibspan.waw.pl

For further volumes:
http://www.springer.com/series/11156

About this Series

The series "Advances in Intelligent Systems and Computing" contains publications on theory, applications, and design methods of Intelligent Systems and Intelligent Computing. Virtually all disciplines such as engineering, natural sciences, computer and information science, ICT, economics, business, e-commerce, environment, healthcare, life science are covered. The list of topics spans all the areas of modern intelligent systems and computing.

The publications within "Advances in Intelligent Systems and Computing" are primarily textbooks and proceedings of important conferences, symposia and congresses. They cover significant recent developments in the field, both of a foundational and applicable character. An important characteristic feature of the series is the short publication time and world-wide distribution. This permits a rapid and broad dissemination of research results.

Advisory Board

Roman Szewczyk · Cezary Zieliński
Małgorzata Kaliczyńska
Editors

Recent Advances in Automation, Robotics and Measuring Techniques

Springer

Editors
Roman Szewczyk
Industrial Research Institute for Automation and Measurements PIAP
Warsaw
Poland

Małgorzata Kaliczyńska
Industrial Research Institute for Automation and Measurements PIAP
Warsaw
Poland

Cezary Zieliński
Industrial Research Institute for Automation and Measurements PIAP
Warsaw
Poland

ISSN 2194-5357 ISSN 2194-5365 (electronic)
ISBN 978-3-319-05352-3 ISBN 978-3-319-05353-0 (eBook)
DOI 10.1007/978-3-319-05353-0
Springer Cham Heidelberg New York Dordrecht London

Library of Congress Control Number: 2014932680

Printed on acid-free paper

Springer is part of Springer Science+Business Media (www.springer.com)

Foreword

Broadly perceived control, automation, robotics and measuring techniques belong to the most relevant fields of science and technology, both from the point of view of theoretical challenges and practical importance. In spite of being separate areas of research, knowledge and expertise, they are strongly related, both in terms of paradigms and tools and techniques employed, as well in terms of their industrial scope of applications. Therefore, an industrial, practice oriented perspective is an important aspects of those areas. Moreover, automation, robotics and measuring techniques have a significant innovative potential as the current industrial practice calls for a further integration of all kinds of production systems, more ecological and energy efficient solutions as well as cost and time effective production and manufacturing processes.

Among many important problems and challenges faced by automation and control, most of which have been reflected in the scope of the papers included in this volume, one can mention, for instance, discrete systems, actuators, diagnostics, and modern tools exemplified by fuzzy logic, evolutionary computation, neural networks, probabilistic approaches, etc.

In robotics, in particular in its part related to the development of mobile robots, one can quote as crucial problems and challenges various problem solving tasks related to the control of walking robots, control of manipulators, motors and drivers, mechatronic systems, and tracking control.

Measuring techniques and systems have to overcome, first of all, barriers implied by environmental conditions and limitations. They call for the development of novel sensors (also utilizing novel materials such as graphene), advanced signal processing and a more foundational development focused on the theory of metrology.

This book presents the recent advances and developments in control, automation, robotics, and measuring techniques that are trying to meet those challenges and to fulfil those technological, economic and social needs. It presents contributions of top experts in the fields, focused on both theory and industrial practice. The particular chapters present a deep analysis of a specific technical problem which is in general followed by a numerical analysis and simulation, and results of an implementation for the solution of a real world problem.

We strongly believe that the presented theoretical results, practical solutions and guidelines will be useful for both researchers working in the area of engineering sciences and for practitioners solving industrial problems.

Warsaw
January 2014

Roman Szewczyk
Cezary Zieliński
Małgorzata Kaliczyńska

Editors

Professor Roman Szewczyk received both his Ph.D. and D.Sc. in the field of mechatronics. He is specializing in the modelling of properties of magnetic materials as well as in sensors and sensor interfacing, in particular magnetic sensors for security applications. He is the leading the development of a sensing unit for a mobile robot developed for the Polish Police Central Forensic Laboratory and of methods of non-destructive testing based on the magnetoelastic effect. Professor Szewczyk was involved in over 10 European Union funded research projects within the FP6 and FP7 as well as projects financed by the European Defence Organization. Moreover, he was leading two regional and national scale technological foresight projects and was active in the organization and implementation of technological transfer between companies and research institutes. Roman Szewczyk is Secretary for Scientific Affairs in the Industrial Research Institute for Automation and Measurements (PIAP). He is also Associate Professor at the Faculty of Mechatronics, Warsaw University of Technology and a Vice-chairman of the Academy of Young Researchers of the Polish Academy of Sciences.

Professor Cezary Zielinski received his M.Sc./Eng. degree in control in 1982, Ph.D. degree in control and robotics in 1988, the D.Sc. (habilitation) degree in control and robotics in 1996, all from the Faculty of Electronics and Information Technology, Warsaw University of Technology, Warsaw, Poland, and Full Professorship in 2012. Currently he is Full Professor both in the Industrial Research Institute for Automation and Measurement (PIAP) and the Warsaw University of Technology, where he is Director of the Institute of Control and Computation Engineering. Since 2007 he has been a member of the Committee for Automatic Control and Robotics, the Polish Academy of Sciences. Professor Zieliński is Head of the Robotics Group in the Institute of Control and Computation Engineering working on robot control and programming methods. His research interests focus on robotics in general and in particular include: robot programming methods, formal approach to the specification of architectures of multi-effector and multi-receptor systems, robot kinematics, robot position-force control, visual servo control, and design of digital circuits. He is the author/coauthor of over 160 conference and journal papers as well as books concerned with the above mentioned research subjects.

Dr. Małgorzata Kaliczyńska received her M.Sc./Eng. degree in cybernetics from the Faculty of Electronics, Wrocław University of Technology, and her Ph.D. degree in the field of fluid mechanics from the Faculty of Mechanical and Power Engineering in this same university. Now she is Assistant Professor in the Industrial Research Institute for Automation and Measurement (PIAP) and Editor of the scientific and technological magazine "Measurements, Automation, Robotics". Her areas of research interest include distributed control systems, information retrieval and webometrics.

Contents

Part I: Control and Automation

Part II: Robotics

Part I
Control and Automation

Application of Artificial Neural Network for Modelling of Electrohydraulic Drive

Mirosław Adamczyk and Andrzej Milecki

Poznan University of Technology
ul. Piotrowo 3, 60-965 Poznań, Poland
M.Adamczyk@iizp.uz.zgora.pl, Andrzej.milecki@put.poznan.pl

Abstract. The article describes the use of the Artificial Neural Network for modelling and simulation of electrohydraulic drive. The investigation test stand for this drive is presented and some investigation results are included. The structure of artificial neural network used for modeling is described and shortly discussed. The teaching procedure is described and some simulation results are presented. The accuracy of simulation results network are included.

Keywords: electrohydraulic drive, artificial neural network, modeling.

1 Introduction

Electrohydraulic servo drives are in their nature non-linear systems and therefore their design and control is not easy. That's why in their design and control, computer modelling methods play very fundamental role. In the literature there are several publications about electrohydraulic drives modelling [1–3]. In most cases the presented models are linear in nature, but only some non-linear blocks are added. In fact not all features of electrohydraulic drives is good enough recognized and described, thus the models and simulation results does not fits very well to characteristic obtained during laboratory investigations.

Neural networks are increasingly employed in a wide range of application such as modelling, control, classification, pattern recognition, signal processing, and may other areas [4, 5]. Feed forward ANN are based on neurons in hidden layers which compute a non-linear function of the scalar product of input vector and a weight vector. There are theoretical justifications that, if the network topology is sufficiently large with sufficient number of hidden layers and neurons, then any continuous function can be approximated by ANN by carefully choosing the parameters of the network [6]. In literature there are publications about applications of artificial neural network in modelling of devices dynamics and in their controllers [7–10]. Therefore authors decided to apply of such networks in modelling of electrohydraulic servo drives. Such models doesn't require the formulation of complicated derivative equations and the transformation them into simulation model. Also knowledge of accurate parameter values is not needed. Instead of special, rather expensive simulation software like, for example MATLAB/Simulink other, also freeware

R. Szewczyk, C. Zieliński, and M. Kaliczyńska (eds.), *Recent Advances in Automation, Robotics and Measuring Techniques*, Advances in Intelligent Systems and Computing 267,
DOI: 10.1007/978-3-319-05353-0_1,

software for neural network simulation software can be used. For preparing the neural network model, the electrohydraulic drive should be investigated at the laboratory test stand and the input and output signals should be recorded. Such investigations results will be then used as learning information for artificial neural network.

It has already been shown that neural network controllers offer advantages over the classical control methods [11–13]. After modelling, the control of the system can be, for example achieved solely by an inverse model of the process [14, 15] or by a combination of both, the inverse and forward models [16].

The most important problem which one faces during design of ANN design and application is the establishment of network structure i.e., number of layers, number of neurons in each layer and activation function of every neuron. At first, these parameters may be established basing on previous research results presented in literature and then corrected during tests. Another important parameter used in data preparation for teaching of ANN is the sampling frequency of the recorded signals. It's common practice that this parameters can be successfully established after several attempts, but one must be aware, that in cases which require high accuracy the selection of ANN parameters may be very difficult [7, 17].

2 Laboratory Tests of Electrohydraulic Drive and Signals Recording

In Figure 1 the scheme diagram and the photo of the test stand are presented. In the research electrohydraulic drive with servo valve with mechanical feedback linkage was used. The output motor was single rod hydraulic cylinder with stroke equal to 400 mm, piston diameter 100 mm and piston rod diameter 60 mm. The cylinder was controlled by servo valve type SM4-20. The drive actuated a lathe table with a mass about 150 kg (see Fig. 1). The actual position was measured with resolution 10 µm by incremental encoder type MSA 6803, which was connected to the computer by special input/output card. The same computer was acting as a servo drive controller i.e. input signal generator. The control and signal recording tasks were performed by DASYLab software, which was installed on the computer.

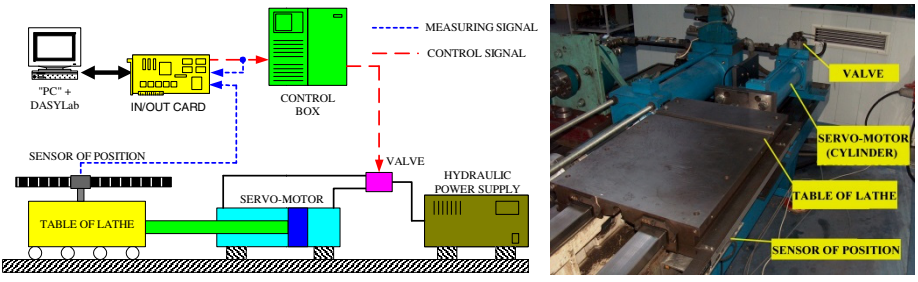

Fig. 1. Test stand: scheme block diagram and a photo

In the computer an input/output card type DaqBoard 3001was installed. The control signal to the servo valve control card was send using 16-bit DA converter, which output voltage was in a range ±10 V. The piston position was measured using two channel (+A, +B) encoder which was worked using following parameters: x4 count mode; latch on scan; pulse detection: edge detect – rising edge, debounce trigger – after stable, debounce time 500 ns. The use of x4 count mode enabled the increase of position measurement resolution to 2 μm. The position was measured on a distance 242 mm, so the maximum number of pulses obtained from encoder was equal to 121 000. The measuring time was equal to 20 sec. The supply pressure was equal to 10 MPa and the fluid temperature was in a range + 55 °C to + 63°C. The servo valve control and the piston position signals were recorded to a files and later transformed to the Matlab-Simulink software.

3 Structure of Artificial Neural Network Used for Modelling

During tests we tried to teach the ANN of different structures using the same training data (signals). The structure of the artificial neural network used in presented here investigations was established after making many time consuming trials. Therefore the obtained results are suitable only for specific electrohydraulic drive and for assumed measurement parameters. In the investigations we used and checkup the usefulness of different three layers ANN structures with input layer: from 4 to 50 artificial neurons with different activation functions and with hidden layer: from 4 to 50 artificial neurons with different activation functions. We tried also different teaching methods and different delays for input signal values (from 2 to 20) and for output signal values (from 2 to 20).

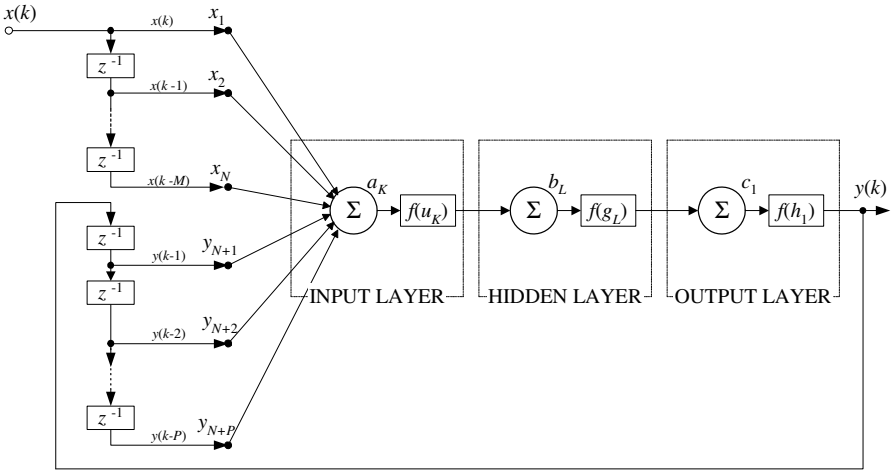

Fig. 2. Simplified scheme diagram of ANN

Finally, we find out the best solutions and decided to use the following ANN structure, which simplified scheme diagram is shown in Fig. 2:

- three layers network with a feedback taken from output,
- input layer: 25 artificial neurons, hyperbolic tangent activation function,
- hidden layer: 35 artificial neurons, hyperbolic tangent activation function,
- output layer: 1 artificial neuron, linear activation function,
- number inputs on which servo drive input signal values are given: 5;
- number inputs on which servo drive output signal values are given: 14;
- delay time for z was equal to 0.01 sec.,
- ANN process time was equal to 0.01 sec.

If we use as input signal the voltage given to servo valve control card and as output signal the piston displacement, then such a drive is modeled in the literature as forth order system connected serially with integrative element [1–3]. So, such a system is asymptotically not stable and therefore cannot be modelled by ANN. Therefore we decided to model a drive with an input signal which was voltage and output signal which was velocity. As input signal the random step-like signal was generated. The output signal was derivative and the average of the last 5 signal values (velocity) are taken for recording, which means that we measured the average velocity for every 0.01 sec. One example of collected signals is shown in Fig. 3.

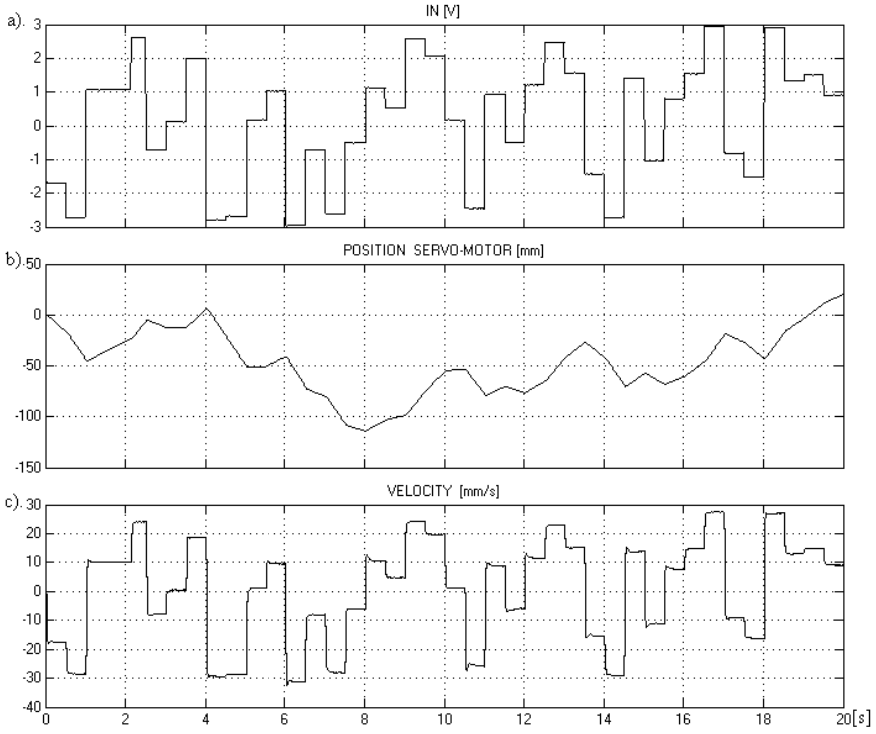

Fig. 3. Signals recorded during electrohydraulic drive investigations: a) servo valve input voltage, b) piston displacement changes, c) average piston velocity (in time 0.01 sec.)

4 Modelling Results and Tests

In teaching process on the artificial neural network inputs, the servo valve input voltage was given and as teaching signal, the piston velocity signal was used. We noticed that in the teaching process, there is optimal number of teaching iterations. In the described here case, it was equal to about 50 iterations. If there were less iterations the ANN was not trained accurately enough. However, if there are more than 50 iterations, the ANN error during teaching process decreased, but after that, when on ANN inputs unknown signal (not used in teaching mode) was given, the error of output signal drastically increased. Therefore in every teaching process we stopped it after 50 iterations.

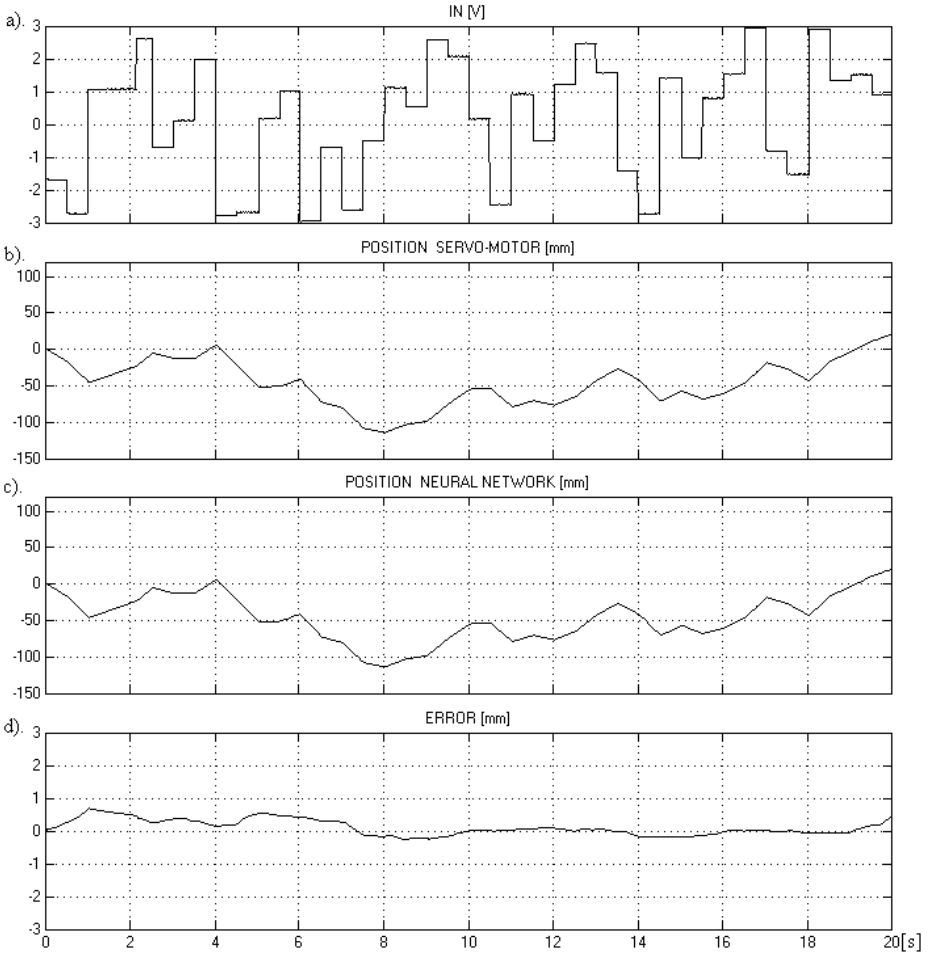

Fig. 4. Signals changes during teaching phase of ANN: a – voltage signal given on valve control card; b – piston position changes; c – ANN responses (position changes); d – ANN error

During the investigations of modelling we also noticed, that on the ANN errors, the values of input and output signals have significant influence. The best solution are obtained when both signals: input and output vary in the same range. The shown in Fig. 3 input signal vary from –3 V to +3 V, but in the same time the output signal vary from –30 mm/sec to +30 mm/sec. Therefore in teaching process, a scaling module was applied, which reduced the velocity signal to ±3 mm/s. On the output of ANN the signal was again rescaled to proper range i.e. ±30 mm/s. These changes are made using MATLAB-Simulink blocks. As mentioned above, the artificial neural network was used to model the velocity changes as a response of voltage on valve electronic card input. Therefore, on the output of ANN an integrator block was added in order to obtain the position on the output. Such a model may be useful in different model based positioning controllers of electrohydraulic servo drive.

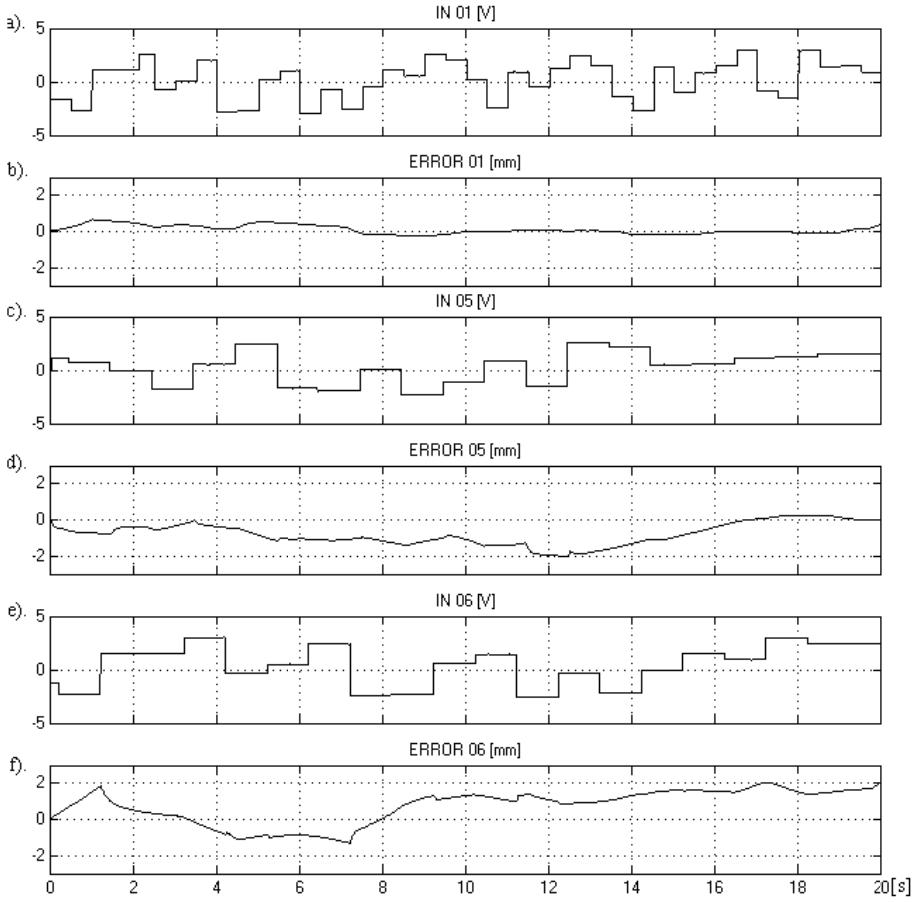

Fig. 5. Simulation results and errors; description see text

For the teaching procedure the signals shown in Fig. 3 were used. During this teaching process we looked for obtainment assumed acceptable position error, which was established in a range of ±1 mm. For comparison, in Fig. 4 signals obtained after teaching process are shown. On the ANN model inputs the same signal as used during teaching was given. One can note, that the ANN output signal is very similar to the output signal of a real drive. Also ANN model error was in acceptable range e.g. less than 1 mm.

In Figure 5 errors of ANN model are shown. At first, the valve input signal, used in teaching is shown (Fig. 5a) and below ANN model error curve obtained during simulations is presented. In Figure 5c and Fig. 5e two other input signals, not used during teaching process, are shown and in Fig. 5d and 5f ANN model error curves obtained during simulation are respectively shown. One can note, that when on the input is the same signal as used during simulation, the modelling error is very low. Unfortunately, when the not known to the ANN input signal is used, the errors are significantly bigger, but the calculated error was always in a range of ±2 mm, which can be regarded as acceptable.

5 Conclusion

The experiments described in the paper showed that the artificial neural networks can be used as effective simulation model of electrohydraulic drive with servo valve. The design of the neural network model does not require a complicated design procedure. Although, usually at a first look it sees that the use of ANN for modelling is very easy, in fact there are several problems to be solved and several questions to be answered. To the most difficult one can regard the choosing of the network architecture, its number of inputs, number of layers, art of activation functions and teaching algorithm. Other questions concern the learning methods and the accuracy and sampling frequency of recorded investigation results. The last factor influence really heavy on accuracy and behavior of artificial neural network model. The results obtained in simulation of electrohydraulic drive shown, that the use of ANN for modelling is possible and gave satisfactory results.

References

1. Merrit, H.E.: Hydraulic Control Systems. John Wiley & Sons, Inc. (1967)
2. Murrenhoff, H.: Servohydraulik. Verlag Meinz, Aachen (1998)
3. Milecki, A.: State space models of electrohydraulic servo. Archives of Mechanical Technology and Automation 23(2) (2003)
4. Haykin, S.: Neural Networks. Macmillan College Publishing Company (1994)
5. Pham, D., Liu, X.: Neural Networks for Identification. Prediction and Control. Springer, Heidelberg (1995)
6. Cybenko, G.: Approximation by superposition of sigmoidal function. Math, Control Signal System (1989)

7. Adamczyk, M., Bachman, P.: Modeling elektrohydraulic elements with the use of artificial neural networks and virtual reality, Virtual design and automation: new trends in collaborative product design. In: Weiss, Z. (ed.) Publishing House of Poznan University of Technology, pp. 485–491 (2006)
8. Ng, G.W.: Application of Neural Networks to Adaptive Control of Nonlinear Systems. Research Studies Press Ltd., London (1997)
9. Yamazaki, K., Chung, J.H.: Application of neural network in mechatronics control, Japan/USA Symp. Flex. Auto. ASME 1, 243–248 (1992)
10. Abdollahi, F., Talebi, H.A., Patel, R.V.: Stable Identification of Nonlinear Systems Using Neural Networks: Theory and Experiments. IEEE/ASME Transactions on Mechatronics 11(4) (2006)
11. Albus, J.S.: A new approach to manipulator control: Cerebellar model articulation control. Trans. ASME, J. of Dyns. Syst., Meas. and Contr. 97, 220–227 (1975)
12. Ito, M.: The Cerebellar and Neural Control. Raven Press, New York (1984)
13. Kawato, M., Uno, Y., Isobe, M., Suzuki, R.: Hierarchical neural network model for voluntary movement with application to robotics. IEEE Contr. Sys. Mag., 8–15 (1988)
14. Psallis, D., Sideris, A., Yamamura, A.: A multilayered neural network controller. IEEE Contr. Syst. Mag., 17–22 (April 8, 1988)
15. Miller, W.T.: Real-time application of neural networks for sensor-based control of robots with vision. IEEE Trans. Syst. Man., Cybern. 19(4), 825–831 (1989)
16. Werbos, P.J.: Backpropagation through time: what it does and how to do it. Proceeding of the IEEE, 1550–1560 (1990)
17. Knohl, T., Unbehauen, H.: Adaptive position control of electrohydraulic servo systems using ANN. Mechatronics 10, 127–143 (2000)

Cyclic Steady State Space Refinement

Grzegorz Bocewicz[1], Zbigniew Banaszak[2], and Paweł Pawlewski[3]

[1] Dept. of Computer Science and Management, Koszalin University of Technology,
Sniadeckich 2, 75-453 Koszalin, Poland
bocewicz@ie.tu.koszalin.pl
[2] Dept. of Business Informatics, Warsaw University of Technology,
Narbutta 85, 02-524 Warsaw, Poland
Z.Banaszak@wz.pw.edu.pl
[3] Dept. of Management Engineering, Poznan University of Technology,
Strzelecka 11, 60-965 Poznan, Poland
pawel.pawlewski@put.poznan.pl

Abstract. A method aimed at refinement of the cyclic steady state space reachable in the given multimodal transportation network is proposed. The paper introduces the concept of a System of Concurrent Multimodal Cyclic Processes in which several subnetworks interact each other via distinguished subsets of common shared workstations as to provide a variety of demand-responsive work-piece transportation/handling services. Searching for the cyclic steady state behavior the following question is considered: Is the cyclic steady state space reachable in the given network structure ? The declarative approach employed makes it possible to evaluate the reachability of cyclic behaviors on a scale that reflects real practice.

Keywords: state space, cyclic steady state, cyclic scheduling.

1 Introduction

The aim of effective management (of a different nature and character) of concurrently executed flows, especially the processes implemented in transport systems, is to make sure that the system behaves in a planned manner which minimizes the operating costs. In terms of the transport system that constitutes a network of multimodal modes of material transport, the aim of logistic management is to select such a structure that guarantees the anticipated variants of traffic at various times of the day as well as during mass events and in crisis situations. It is quite obvious that various behaviors of the system and, as a result, the implementations of various variants of a journey are determined by the parameters of a transport structure, such as the number and length of particular lines, number of modes of transport as well as limitations related with their capacity and speed.

In general terms, it means that various structures of a transport system may produce different variants of its performance, especially divergent scenarios of the traffic control in transport. In the presented context, it seems necessary to evaluate and, consequently, to prepare variants of a potential multimodal structure of a transport network, e.g. in the

R. Szewczyk, C. Zieliński, and M. Kaliczyńska (eds.), *Recent Advances in Automation, Robotics and Measuring Techniques*, Advances in Intelligent Systems and Computing 267,
DOI: 10.1007/978-3-319-05353-0_2,

phase of its design or modernization. The present work focuses on this problem. The accepted model assumes there is a network of concurrently implemented cyclic processes (modes of transport) that use commonly available resources (elements of routes, stops, stations etc.). The local cyclic processes, synchronized with a protocol of mutual exclusion, make it possible to implement the so-called multimodal processes, i.e. processes understood as material flow traffic in particular directions (e.g. east- west) or between the selected points in the network. For such a model, it is crucial to find a method of prompt variant preparation for the particular structures and organization of material transport multimodal networks.

The problems of evaluating the cyclic implementation of processes are usually considered in terms of cyclic scheduling problems. The literature on the subjects provides numerous methods of solving these problems [5]. Among them there are mathematic programming methods [1, 10], max-plus algebra methods [6], constraint programming techniques [3, 4], Petri nets [9], etc. Most of them deal with seeking solutions than minimize the period of cyclic scheduling. The approaches that make it possible to evaluate cyclic behaviors and, at the same time, avoid deadlocks are quite rare. Therefore, the presented method makes it possible to determine the non-blocking behaviors (i.e. cyclic schedules) in the systems of concurrently executed multimodal processes.

Section 2 provides a description of the System of Concurrent Multimodal Cyclic Processes (SCMCP) – model of a structure and behavior of the considered class of multimodal network of material transport. Automated Guide Vehicle System (AGVS) is considered as a real-life case of the multimodal network composed of different components such as lifts, AGVs, transporters and so on. In Section 3 we formulate the problem of prompt prototyping of behaviors observed in the given structure of the multimodal network. The method of solving this problem is shown in Section 4. Then, Sections 5 and 6 describe the conducted experiments and provide conclusions resulting from them.

2 System of Concurrent Multimodal Cyclic Processes

2.1 Structure

Fig. 1 shows an example of a AGVS structure of which is a composition of numerous recurring fragments (subsystems): the material transport takes place within them. Work pieces are transported along two set routes: north-south (blue line – mP_1) and east-west (red line – mP_2). These routes, setting the courses of multimodal processes, are composed of fragments of the proper lines of transport (AGV routes). In the considered case, there are four AGV lines (P_1, P_3, P_2 and P_4) used to transport materials along the routes. A system of this kind can be modeled as the SCMCP shown in Fig. 2a). The class SCMCP is assumed to include two types of processes:

- *local processes* (representing modes of transport – P_1, P_2, P_3, P_4), whose operations are cyclically repeated along the set routes (sequences of successively used resources). For the system from Fig. 2a), the routes of local processes are defined as follows:

$$p_1 = (R_6, R_2, R_3),\ p_2 = (R_5, R_1, R_2),\ p_3 = (R_4, R_1, R_8),\ p_4 = (R_3, R_4, R_7),$$

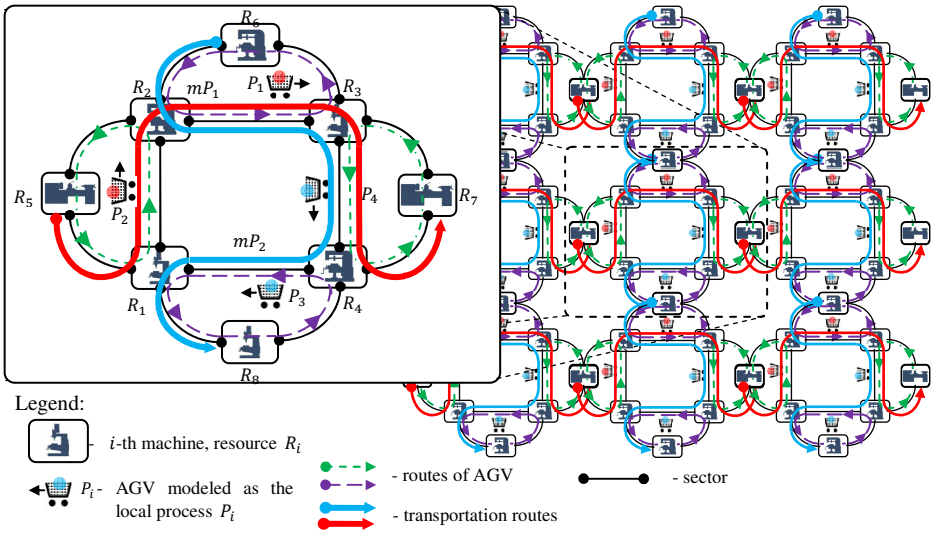

Fig. 1. Example of an AGVS

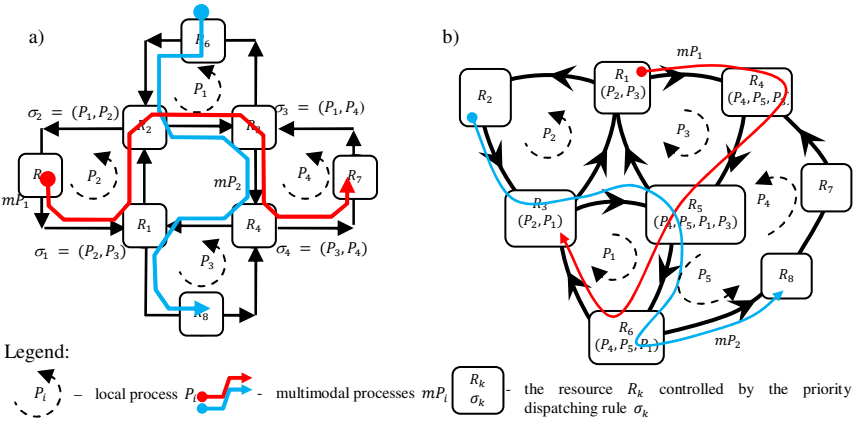

Fig. 2. SCMCP model of an AGVS from: Fig 1 a), and for an example from Fig. 3 b)

- *multimodal processes* (mP_1, mP_2) representing streams of materials. Operations of the multimodal processes are implemented cyclically along routes being compositions of fragments of routes of local processes representing resources used for transporting materials along a given route. For the system from Fig. 2a), the routes of multimodal processes are defined as follows:

$$mP_1 = \big((R_5, R_1, R_2), (R_2, R_3), (R_3, R_4, R_7)\big),$$
$$mP_2 = \big((R_6, R_2, R_3), (R_3, R_4), (R_4, R_1, R_8)\big).$$

Process operation are implemented on two kinds of resources: own resources (each of them is used by only one process of a given kind – R_5, R_6, R_7, R_8) and shared

resources (each of them is used by more than one process of a given kind – R_1, R_2, R_3, R_4). Process uses resources that are shared in the mode of mutual exclusion, i.e. in a given moment only one process operation of a given kind can be implemented on a resource (yet, process operations of different kinds, local and multimodal, can be implemented simultaneously).

The access to shared resources is given in the sequence determined by the dispatching rules $\Theta = \{\Theta^0, \Theta^1\}$. It is assumed that $\Theta^l = \{\sigma_1^l, \ldots, \sigma_k^l, \ldots, \sigma_{lk}^l\}$, where σ_k^l – is the sequence whose elements determine the order in which the processes (local $l = 0$ / multimodal $l = 1$) are provided with access to the resource R_k. In case of the system from Fig. 2a), the access to shared resources is determined by the following rules

$$\sigma_1^0 = (P_2, P_3),\ \sigma_2^0 = (P_1, P_2),\ \sigma_3^0 = (P_2, P_3),\ \sigma_4^0 = (P_3, P_4),$$
$$\sigma_1^1 = (mP_2, mP_1),\ \sigma_2^1 = (mP_1, mP_2),\ \sigma_3^1 = (mP_1, mP_2),\ \sigma_4^1 = (mP_2, mP_2).$$

The subsequent operation starts right after the current operation is completed, providing that the resource indispensible to its implementation is available. While waiting for the busy resource, the process does not release the resource which was assigned for implementing the previous operation. Moreover, an assumption is made that processes are of no-expropriation nature, and the times and sequence of operations performed by the processes do not depend on external interferences.

The parameters described above constitute the structure of SCMCP that determines its behavior. Formally, the structure of SCMCP is defined as the following tuple [3]:

$$SC = \big((R, SL), SM\big)\ , \tag{1}$$

where: $R = \{R_k \mid k = 1, \ldots, lk\}$ – set of resources,

$SL = (P, U, O, T, \Theta^0)$ – structure of local processes, where:

- $P = \{P_i \mid i = 1 \ldots ln\}$ – set of local processes , P_i – i^{th} process,
- $U = \big\{p_i = \big(p_{i,1}, \ldots, p_{i,j}, \ldots, p_{i,lr(i)}\big) \mid i = 1 \ldots ln\big\}$ – set of routes of local processes, p_i – i^{th} route, $p_{i,j} \in R$ – resource required for implementing j^{th} operation of the process P_i,
- $O = \big\{O_i = \big(o_{i,1}, \ldots, o_{i,j}, \ldots, o_{i,lr(i)}\big) \mid i = 1 \ldots ln\big\}$ – set of sequences of operations, $o_{i,j}$ – j^{th} operation of the process P_i,
- $T = \big\{T_i = \big(t_{i,1}, \ldots, t_{i,j}, \ldots, t_{i,lr(i)}\big) \mid i = 1 \ldots ln\big\}$ – set of sequences of operation performance times, $t_{i,j}$ – time of performing an operation $o_{i,j}^h$,
- $\Theta^0 = \big\{\sigma_k^0 = (s_{k,1}^0, \ldots, s_{k,d}^0, \ldots, s_{k,lh(k,0)}^0) \mid k = 1 \ldots lk\big\}$ – set of dispatching rules, σ_k^0 – dispatching rule for the resource R_k, $s_{k,d}^0$ – local process, $lh(k, 0)$ – length of the rule σ_k^0,

$SM = (mP, mU, mO, mT, \Theta^1)$ – structure of multimodal processes, where:

- $mP = \{mP_i \mid i = 1 \ldots lw\}$ – set of multimodal processes mP_i, lw- number of the processes
- $mU = \big\{mp_i = \big(mp_{i,1}, \ldots, mp_{i,j}, \ldots, mp_{i,lm(i)}\big) \mid i = 1 \ldots lw\big\}$ – set of routes of local processes, mp_i – i^{th} route,

$mO = \{mO_i^h = (mo_{i,1}, \ldots, mo_{i,j}, \ldots, mo_{i,lm(i)}) \mid i = 1 \ldots lw\}$ – set of sequences of operations, $mo_{i,j}$ – j^{th} operation of the process mP_i,

$mT = \{mT_i = (mt_{i,1}, \ldots, mt_{i,j}, \ldots, mt_{i,lm(i)}) \mid i = 1 \ldots lw\}$ – set of sequences of operation times, $mt_{i,j}$ – time of operation performance $mo_{i,j}$,

$\Theta^1 = \{\sigma_k^1 = (s_{k,1}^1, \ldots, s_{k,d}^1, \ldots, s_{k,lh(k,1)}^1) \mid k = 1 \ldots lk\}$ – set of dispatching rules of multimodal processes, σ_k^1 – dispatching rule for the resource R_k, $s_{k,d}^1$ – multimodal process, $lh(k,1)$ – length of the rule σ_k^1.

2.2 Behavior

In the systems of concurrent cyclic processes, the behavior is usually presented [5], [6], as schedules determining the moments of initiating all the operations implemented within them. Fig. 3a) provides an example of such a schedule that determines the way of implementing the processes of SC structure from Fig. 2b).

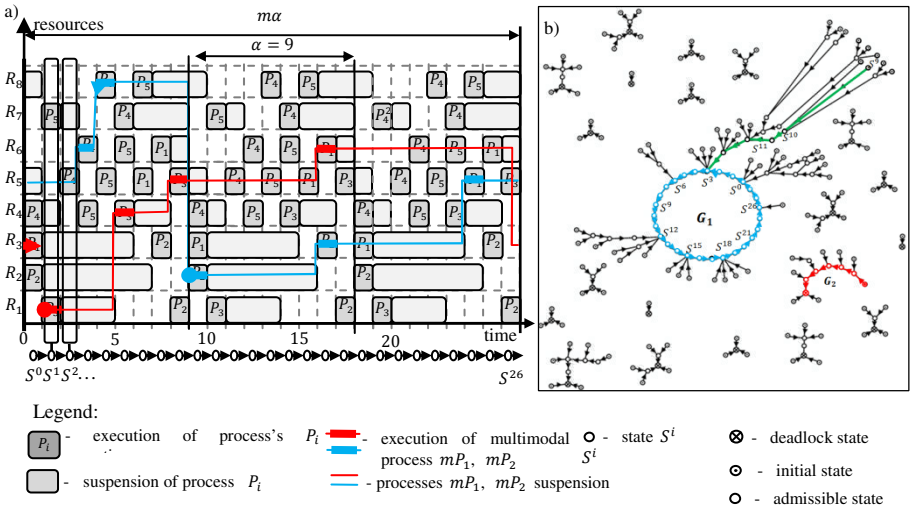

Fig. 3. Cyclic schedule for structure from Fig. 2b) a), and the corresponding states space $\mathcal{P}$ b)

The presented schedule is an example of cyclic behavior, i.e. the successive states of the processes are reachable with the constant period (the operations of local processes are repeated with the period $\alpha = 9$ t.u. (time units) and the multimodal processes with $m\alpha = 27$ t.u.

In this approach, each behavior can be comprehended as a sequence of successive states (subsequent allocations of processes, as well successively changing, according to the rules Θ of access rights). In case of the schedule from Fig. 3a), it is a sequence of 27 states $S^0, S^1, S^2, \ldots, S^{26}$. Formally the SCMCP state is defined as follows [3]:

$$S^r = (Sl^r, mS^r), \tag{2}$$

where Sl^r means the r^{th} state of local processes:

$$Sl^r = (A^r, Z^r, Q^r),$$

$A^r = ({a_1}^r, {a_2}^r, \ldots, {a_k}^r, \ldots, {a_{lk}}^r)$ – **allocation** of local processes In the r^{th} state, ${a_k}^r \in P \cup \{\Delta\}$; ${a_k}^r = P_i$ – **allocation** meaning that the resource R_k occupied by the process P_i, and ${a_k}^r = \Delta$ – means that the resource R_k is unoccupied.

$Z^r = ({z_1}^r, {z_2}^r, \ldots, {z_k}^r, \ldots, {z_m}^r)$ – **sequence of semaphores** of the r^{th} state, ${z_k}^r \in P$ – **semaphore** determining the process (an element of rule σ_k^0), which has an access to the resource R_k next in the sequence, i.e. ${z_k}^r = P_i$ means that process P_i is the next to access the resource R_k .

$Q^r = ({q_1}^r, {q_2}^r, \ldots, {q_k}^r, \ldots, {q_m}^r)$ – **sequence of semaphore indexes** of the r^{th} state, ${q_k}^r$ – **index** determining the position of the semaphore value ${z_k}^r$ in the dispatching rule σ_k^0, ${z_k}^r = s_{k,({q_k}^r)}$, ${q_k}^r \in \mathbb{N}$. For example, ${q_2}^r = 2$ and ${z_2}^r = P_1$ means that the process P_1 is the second element of the dispatching rule σ_2^0.

mS^r means the r^{th} state of multimodal processes:

$$mS^r = (mA^r, mZ^r, mQ^r),$$

$mA^r = ({ma_1}^r, {ma_2}^r, \ldots, {ma_k}^r, \ldots, {ma_m}^r)$ – sequence of multimodal processes allocation in the r^{th} state, ${ma_k}^r \in mP \cup \{\Delta\}$,

$mZ^r = ({mz_1}^r, {mz_2}^r, \ldots, {mz_k}^r, \ldots, {mz_m}^r)$ – sequence of semaphores of the r^{th} state, ${mz_k}^r \in mP$ – determines the process (an element of the rule σ_k^1, ascribed to R_k), which has the access right to the resource R_k,

$mQ^r = ({mq_1}^r, {mq_2}^r, \ldots, {mq_k}^r, \ldots, {mq_m}^r)$ – sequence of semaphore indexes of the r^{th} state, ${mq_k}^r$ determines the position of the semaphore value ${mz_k}^r$ in the dispatching rule σ_k^1, ${mz_k}^r = s_{k,({mq_k}^r)}$, ${mq_k}^r \in Z$.

Behaviors of the system characterized by various sequences of subsequently reachable states S^r (2) can be illustrated in a graphical form as a state space $\mathcal{P}$. Fig. 3b) shows an example illustrating this possibility for the system from Fig. 2b). If we take the graph-theoretical interpretation of the space $\mathcal{P}$ the diagraph corresponding to it is represented by the pair $\mathcal{P} = (\mathbb{S}, \mathbb{E})$, where $\mathbb{S}$ means a set of admissible SCMCP states [3], $\mathbb{E} \subseteq \mathbb{S} \times \mathbb{S}$ means a set of arcs representing transitions between SCMCP states (transitions take place according to the function $S^f = \delta(S^e)$ described in [3].

Cyclic behaviors shown in Fig. 3b) are connected with the presence of cyclic subgraphs (e.g. digraph G_1) in the space $\mathcal{P}$. The initiation of process implementation from an arbitrary state of the digraph G_1 results in attaining (e.g. by means of transition states) the states being part of a cycle (states marked with blue). A set of such sates depicted by a cyclic route is called as a **cyclic steady state**.

It must be emphasized that not all of the state space $\mathcal{P}$ result in such a cyclic steady states. Most states lead to deadlock states (marked with the symbol ⊗), which in practice mean an interrupt of the system resulting from the occurrence of a closed chain of requests (e.g. blockade of AGV lines caused by AGV stops occupancy).

In general case the space $\mathcal{P}$ may not include cyclic steady states. Such situations are quite common in the systems with high density of processes (e.g. in transportation systems). In the context of such systems, the question of evaluating the cyclic behavior attainability becomes crucial.

3 Problem Formulation

There is SCMCP with the structure SC (1) including:

- set of resources R,
- local processes P described by routes p_i, operation sequences O_i and their duration times T_i,
- multimodal processes mP dscribed by the routes mp_i, operation sequences mO_i and their duration times mT_i,
- set of dispatching rules Θ.

An answer is sought to the question: Is the space $\mathcal{P}$ of determined cyclic steady states reachable in the SCMCP system with the given structure ?

A positive answer to this question implicates other issues concerning the period of the reachable cyclic steady states, the degree to which the resources are used, methods of transitions between the determined cyclic steady states, the method of avoiding internal disturbances (e.g. breakdowns of modes of transport or traction failures) etc.

4 Method of Generating the State Space

In order to answer the question posed above, we have developed an approach that uses the following properties of the pace of states $\mathcal{P}$ [3]:

1. initial state (in Fig. 3b) marked with the symbol $\odot$) is a state without input arcs, $SB \subseteq \mathbb{S}$ – means a set of all initial states of the space $\mathcal{P}$,
2. deadlock state ($\otimes$) is a state without output arcs,
3. if in the space $\mathcal{P}$ there is a non-empty set of states $\mathbb{S} \neq \emptyset$, in which no state is an initial state $SB = \emptyset$, then all the states are included into cyclic steady states.

The proposed approach is based on the idea of the iterative elimination of the initial states SB out of the states space $\mathcal{P}$, which is illustrated by the example below.

In a set of acceptable states $\mathbb{S}$, of the system with the structure SC, let there be a non-empty subset of initial states $SB_{(1)} \neq \emptyset$ – where the subscript refers to the number of successively implemented steps of the proposed procedure. In the first step, it is assumed that all states $SB_{(1)}$ are inadmissible. It means that constraints excluding states $SB_{(1)}$ are added to constraints determining admissibility. Therefore, a new set $\mathbb{S}_{(1)} \subset \mathbb{S}$ is obtained and it is devoid of initial states $\mathbb{S}_{(1)} \cup SB_{(1)} = \mathbb{S}$. In the graph representation, it means that all digraphs of the space $\mathcal{P}$ have been reduced by the initial states – and that leads to the space $\mathcal{P}_{(1)}$.

It is easily noticeable that the elimination of initial states results in shortening all the transitory routes, and each descendant of the initial state of the space $\mathcal{P}$ becomes an initial state of the space $\mathcal{P}_{(1)}$.

In the subsequent state, a set of initial states $SB_{(2)}$ is determined again, this time, however, in the set of states $\mathbb{S}_{(1)}$ (set of states of the space $\mathcal{P}_{(1)}$). If $SB_{(2)}$ is a non-empty set $SB_{(2)} \neq \emptyset$ then, similarly as in the first step, they are considered inadmissible states. As a result of the reduction of states of the set $SB_{(2)}$, another set

$\mathbb{S}_{(2)} \subset \mathbb{S}_{(1)}$ is obtained (along with the space $\mathcal{P}_{(2)}$) and the whole procedure is repeated all over again for it. The content of the set of initial states is checked by the stop condition. If in the ith state, the set of initial states is empty $SB_{(i)} = \emptyset$, then according to the property (iii), each state of the set $\mathbb{S}_{(i-1)}$ (providing the set is not empty) is a state included into the cyclic steady states. The set $\mathbb{S}_{(i-1)}$ thus obtained is a subset $\mathbb{S}$ consisting only of states included in the steady cyclic steady states.

The stage of determining the set of initial states plays a crucial role in the presented procedure. Therefore, a fundamental question arises concerning the method of determining the sets $SB_{(i)}$. The set $SB_{(i)}$ may be considerd as a set of all solutions to the following the constraints satisfaction problem [3, 8]:

$$PS_{SB(i)} = \left((S^r, D_S), C_{SB(i)}\right), \tag{3}$$

where: S^r – decision variable, initial state $S^r \in \mathbb{S}$,

D_S – domain determining admissible values of variables (allocation, semaphores, indexes) characterizing the state S^r,

$C_{SB(i)} = C_N \cup \{S^r \neq \delta(S^e), \forall S^e \in \mathbb{S}\} \cup C_{SB}(i-1)$ – set of constraints:

C_N – constraints of admissibility of states S^r [3],

$\{S^r \neq \delta(S^e), \forall S^e \in \mathbb{S}\}$ – constraint that guarantees that S^r is an initial state (there is no state S^e leading to state S^r).

$C_{SB}(i-1) = \{S^r \notin SB_{(1)}, S^e \notin SB_{(1)}, S^r \notin SB_{(2)}, S^e \notin SB_{(2)}, \dots, S^r \notin SB_{(i-1)}, S^e \notin SB_{(i-1)}\}$ – a set of constraints excluding initial states determined in the steps $1 \dots (i-1)$ out of the set of solutions.

A solution to the problem $PS_{SB(i)}$ (3) is the admissible state S^r that no other admissible state S^e: $S^r \neq \delta(S^e), \forall S^e \in SB$ leads to. The state S^r determined in this way meets the assumptions of the initial state (i). Therefore, the set of all thus determined solutions to the problem $PS_{SB(i)}$ is the set $SB_{(i)}$. It means that with use of this problem in the iterative procedure (solution to the problem (3) successively for $i = 1,2,3 \dots$) it is possible to determine a set of states constituting all cyclic steady states of the system. The applied algorithm has the following form:

Algorithm 1

function CyclicSteadyStateGeneration(D_S, C_N, δ)

$i \leftarrow 0 \quad C_{SB}(0) \leftarrow \emptyset$

do $i \leftarrow i + 1$

$PS_{SB(i)} \leftarrow \left((S^r, D_S), C_N \cup \{S^r \neq \delta(S^e), \forall S^e \in \mathbb{S}\} \cup C_{SB}(i-1)\right)$

$SB_{(i)} \leftarrow$ SearchAll$(PS_{SB(i)})$

$C_{SB}(i) \leftarrow C_{SB}(i-1) \cup \{S^r \notin SB_{(i)}, S^e \notin SB_{(i)}\}$

while $SB_{(i)} \neq \emptyset$

$PS_C \leftarrow \left((S^r, D_S), C_N \cup C_{SB}(i)\right)$

$V \leftarrow$ SearchAll(PS_C)

return $V(DC)$

end

where:

D_S, C_N, δ – input data, defined as in (3), $PS_{SB(i)}$ – problem of meeting the constraints (3), $SB_{(i)}$ – set of initial states of the ith step,
V – set of states constituting all cyclic steady states of the space $\mathcal{P}$.
SearchAll(PS) – function returning the set of all solutions to the problem PS (in case of no solution the function returns a empty set) .

The input data for the Algorithm 1 are constraints of admissibility of states C_N, transition function δ and the domain D_S determining values of variables describing states of the system. Each of these values is determined by the accepted form of the structure SC (1) of SCMCP. The set of cyclic steady states V, which does not include initial states, is the result returned by the algorithm.

5 Computational Experiment

Consider a system from Fig. 2a) that represents a transport subsystem of the network from Fig. 1. In the system, transport of materials takes place along routes: north-south and west-east (multimodal processes: mP_1, mP_2).

For thus defined system an answer is sought to the question whether in the system from Fig. 2a) cyclic transport of materials is possible (by modes of local processes P_1, P_2, P_3, P_4). In order to determine all possible cyclic steady states we used Algorithm 1. In the considered case it required the realization of four steps (solving problems $PS_{SB(1)}$, $PS_{SB(2)}$, $PS_{SB(3)}$, PS_C). The total time of calculations was no longer than 3 seconds (Oz Mozart, Windows 7, Intel Core Duo2 3.00 GHz, 4 GB RAM). The obtained state space is illustrated in Fig. 4a). It is clear that there are five cyclic steady states $D_{C,1}, D_{C,2}, \ldots, D_{C,5}$ reachable in the system.

It means that the analyzed system can work in five modes characterized by various periods of process implementation and, as a result, by different times of passenger transport. In other words, in SCMCP from Fig. 2a) five various forms of behavior are

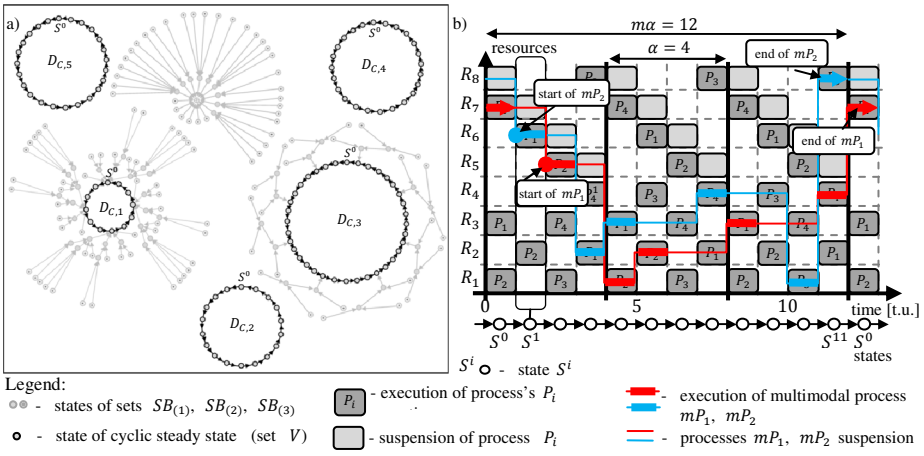

Fig. 4. The state space of SCMCP from Fig. 2a), cyclic schedule for the route $D_{C,1}$

reachable. The periods of the obtained cyclic steady states amount to 12, 18, 36, 24 and 24 t.u. In order to guarantee the shortest transport times, the implementation of processes according to route $D_{C,1}$ should be applied. An example of a schedule corresponding to this route is shown in Fig. 4b).

6 Conclusions

The presented method of prompt prototyping of cyclic steady state space $\mathcal{P}$ (i.e. the states reachable in the given structure of the system), is one of the computer-assisted methods of creating different variants of multimodal networks. The use of the declarative approach makes it possible to evaluate the reachability of cyclic behaviors on a scale that reflects real practice (in the considered case the calculation time was no longer than 3 seconds).

The real-life cases of multimodal networks are strongly affected by the imprecise character of available information (such as time duration, moment of initiation, etc.). The presented expectations specify the development directions for the presented model and method, providing a possibility of taking into consideration the imprecise character of decision variables, e.g. within the Fuzzy Constraints Satisfaction Problem [2, 7] framework.

References

1. Abara, J.: Applying integer linear programming to the fleet assignment problem. Interfaces 19, 4–20 (1989)
2. Bach, I., Bocewicz, G., Banaszak, Z., Muszyński, W.: Knowledge based and CP-driven approach applied to multi product small-size production flow. Control and Cybernetics 39(1), 69–95 (2010)
3. Bocewicz, G., Banaszak, Z.: Declarative approach to cyclic steady state space refinement: periodic process scheduling. The International Journal of Advanced Manufacturing Technology 67(1-4), 137–155 (2013)
4. Bocewicz, G., Wójcik, R., Banaszak, Z.: Multimodal processes scheduling in mesh-like networks composed of periodic systems. In: Grzech, A., Borzemski, L., Świątek, J., Wilimowska, Z. (eds.) Information Systems Architecture and Technology, Networks Design and Analysis, Wrocław, pp. 65–76 (2013)
5. Levner, E., Kats, V., Alcaide, D., Pablo, L., Cheng, T.C.E.: Complexity of cyclic scheduling problems: A state-of-the-art survey. Computers & Industrial Engineering 59(2), 352–361 (2010)
6. Polak, M., Majdzik, P., Banaszak, Z., Wójcik, R.: The performance evaluation tool for automated prototyping of concurrent cyclic processes. Fundamenta Informaticae 60(1-4), 269–289 (2004)
7. Relich, M.: A declarative approach to new product development in the automotive industry. In: Environmental Issues in Automotive Industry, EcoProduction, pp. 23–45 (2014)
8. Sitek, P., Wikarek, J.: A hybrid method for modeling and solving constrained search problems. In: Federated Conference on Computer Science and Information Systems (FedCSIS), pp. 385–392 (2013)
9. Song, J.-S., Lee, T.E.: Petri net modeling and scheduling for cyclic job shops with blocking. Computers & Industrial Engineering 34(2), 281–295 (1998)
10. Von Kampmeyer, T.: Cyclic scheduling problems, Ph.D. Dissertation, Fachbereich Mathematik/Informatik, Universität Osnabrück (2006)

Using Fuzzy Logic for Improving the Control Performance of Digital Servo Drives with Elastic Coupling

Bogdan Broel-Plater

Faculty of Electrical Engineering, West Pomeranian University of Technology, Szczecin
Bogdan.Broel-Plater@zut.edu.pl

Abstract. In the paper a method for improving the control performance for a typical digital servo drive with a torsionable lead-screw and nonlinear static friction is presented. The method is based on employing an additional feedback the operational intensity of which is determined by means of fuzzy logic. Computer simulations show that the presented solution provides high control accuracy for motions at velocities close to zero and stepwise changes in the position set-point.

Keywords: servo drive, control performance, lead-screw, PI controller, elastic coupling.

1 Introduction

The tool motion control accuracy relative to the workpiece over a wide speed range determines the class of CNC machine tools [3, 9]. Among the most important factors that hinder achieving the high accuracy of the motion mention can be made of variations in mass and moments of inertia of moving objects, backlash and torsionability of lead-screws used in classic machine tool axes [3,9]. Additionally, the control performance is strongly affected by the nonlinear static friction while moving with small varying speeds. That is the reason why work on control algorithms that would improve performance of digital servo drives is still underway [4, 6, 8, 10].

Performance of a servo drive can be assessed by means of different criteria. However for machine tool servo drives the most important goal is to reach the desired position as quick as possible without any overshoot and to maintain that position without any oscillations. Only compliance with these requirements, especially for small speeds and minimal stepwise changes in the position set-point, makes it possible to perform a precise machining and micromachining [2, 3, 9].

In the paper a simple algorithm that provides a significant improvement in the control accuracy of slow motions carried out by a servo drive with a torsionable lead-screw and nonlinear static friction. The presented algorithm is an extension of that described in [2], which minimizes the effect of static friction on the control accuracy of a typical digital servo drive.

R. Szewczyk, C. Zieliński, and M. Kaliczyńska (eds.), *Recent Advances in Automation, Robotics and Measuring Techniques*, Advances in Intelligent Systems and Computing 267,
DOI: 10.1007/978-3-319-05353-0_3,

The solution presented in the paper has been validated by means of a computer simulated operation of the ACOPOS digital servo drive manufactured by Bernecker & Rainer [1].

2 Basic Structure of the ACOPOS Servo Drive

In a classic servo drive the axially directed motion is governed by a cascade of controllers responsible for position (RX), velocity (RV) and current (RI). In the ACOPOS digital servo drive we have to do with anti-windup PI controllers [1]. In the position controller (RX) of the servo drive use also can be made of an additional feed-forward control. The structure of the servo drive and its component controllers is shown in Figs. 1 – 4.

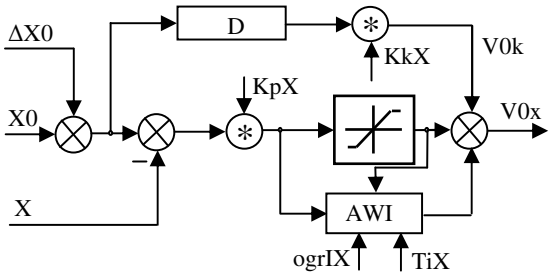

Fig. 1. Structure of the position controller (RX) used in the ACOPOS servo drive: AWI – anti-windup integrator, D - differentiator, X0 and ΔX0 – basic and auxiliary set-point, X – controlled position, V0x – controller output, V0k – velocity-related feed-forward signal, KkX, KpX, ogrIX and TiX – position controller settings

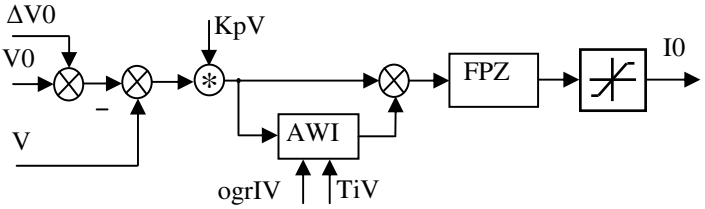

Fig. 2. Structure of the velocity controller (RV) used in the ACOPOS servo drive: AWI – anti-windup integrator, FPZ – band-elimination filter, V0 and ΔV0 – basic and auxiliary set-point, V – controlled velocity, I0 – controller output, KpV, ogrIV and TiV – velocity controller settings

The algorithm of the position controller in the ACOPOS servo drive is repeated every 400 μs, that of the velocity controller every 200 μs, and that of the current controller every 100 μs. With the same frequency the parameter values of any of four controllers also can be altered. This makes it possible to employ the described algorithm to improve the performance of the servo drive.

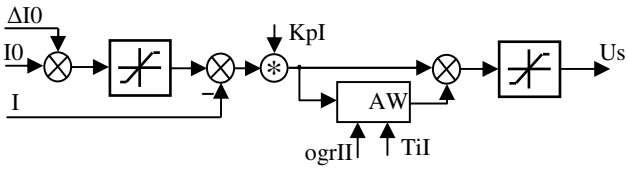

Fig. 3. Structure of the current controller (RI) used in the ACOPOS servo drive: AWI – anti-windup integrator, I0 and ΔI0 – basic and auxiliary set-point, I – controlled current drawn by the motor, Us – controller output, KpI, ogrII and TiI – current controller settings

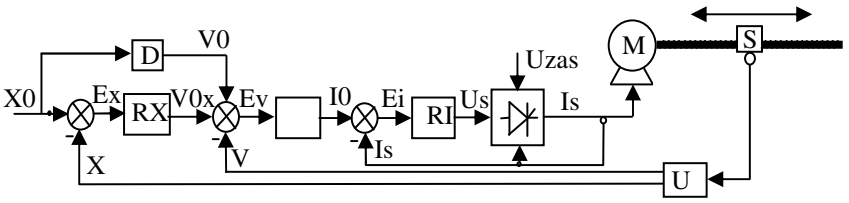

Fig. 4. Output structure of the simulated servo drive: RX, RV, RI – controllers of position, velocity and current respectively, the structure of which is shown in Figs. 1-3, UP – position and velocity measurement system, M – servo drive motor, S – machine tool slide, X0 – slide reference position, V0x, I0 – outputs of position and velocity controllers, Us – current controller output, I – current drawn by the motor, Uzas – supply voltage; the remaining symbols as in Figs. 1-3

3 Motor and Load Model of the Servo Drive

Machine tool servo drives must provide high control accuracy over a wide range of velocities and accelerations. The resultant moment of inertia (Jp) and braking torque (Mh) varying in the process of operation, controller nonlinearities, static friction and dynamic constraint imposed on the current drawn by the servo drive motor make it impossible to optimize effectively the servo drive operation only on the basis of a theoretical analysis. Therefore, computer simulations have been invoked to improve the servo drive performance. Analysis of results obtained enables one to develop a fuzzy algorithm that improves the control performance of the servo drive with a torsionable lead-screw.

In the computer-assisted servo drive simulation a model of a DC motor, shown in Fig. 5, with permanent magnets and an electronic power supply block that constraints the rotor current intensity [5] has been used.

In Figs. 6, 7 and 8 characteristics of the relative driving torque for the modeled motor and those of its own relative braking torque and the relative braking torque referred to the motor shaft produced by the machine tool slide are displayed. These characteristics are related to the maximum resultant braking torque.

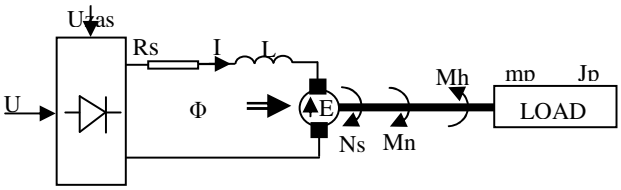

Fig. 5. Equivalent diagram of the motor along with the control block used during tests; Us – manipulated variable, Uzas – supply voltage, mp i Jp – displaced mass and its moment of inertia referred to the motor axis, Ns – rotational speed of the motor, Mn and Mh – driving and braking torques, Φ and Es – magnetic flux and induced counter-electromotive force, R and L – resistance and inductance of the rotor circuit, I – current in the rotor circuit

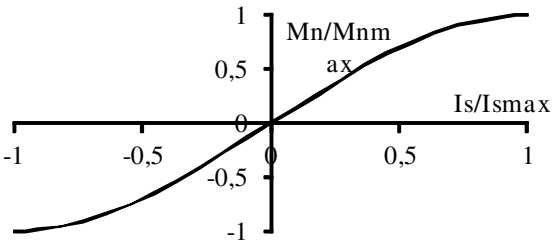

Fig. 6. Characteristic of the relative driving torque developed by the motor as a function of the relative current drawn by the motor

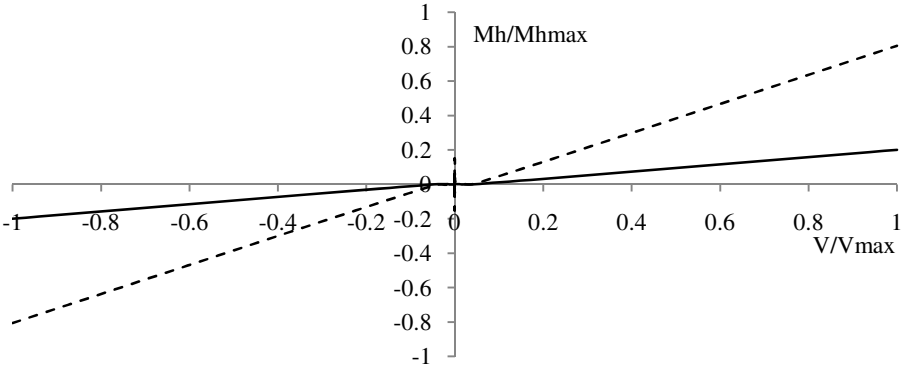

Fig. 7. Full characteristic of the relative braking torque as a function of the relative velocity developed by the motor; solid line – characteristic of the motor self-braking torque, broken line – characteristic of the slide braking torque referred to the motor axis

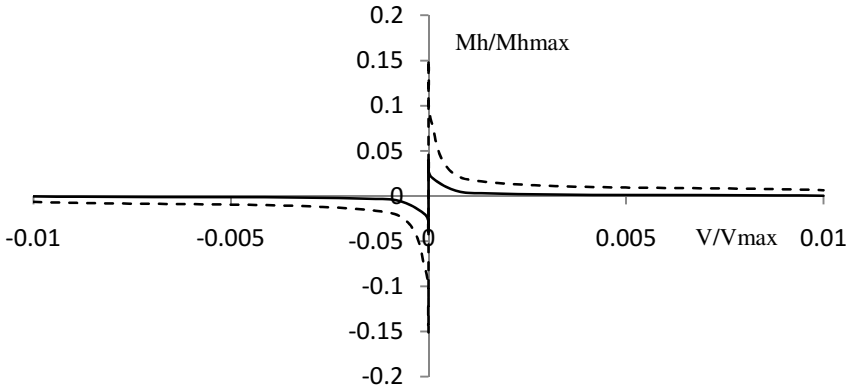

Fig. 8. Relationship between the relative static braking torque of the motor and its relative velocity – a fragment of characteristics of Fig. 7 enlarged for the lowest velocities

Figure 9 shows the torsion of the lead-screw being referred to the motor shaft and dependent on the slide position, at which the static braking torque hindering the machine tool slide motion is overcome and the slide motion starts.

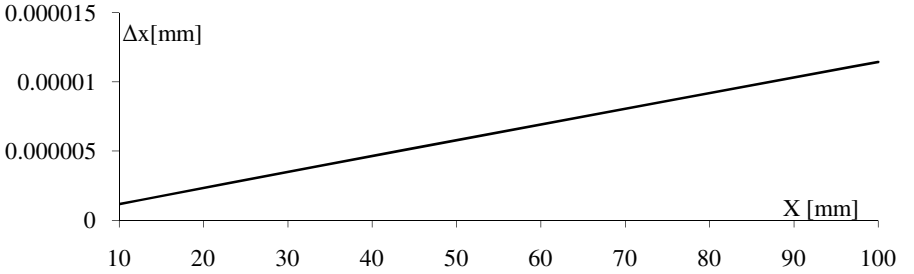

Fig. 9. Characteristic of the lead-screw torsion referred to the motor axis, at which the slide motion starts

4 Algorithm for Improving the Motion Control Accuracy of a Servo Drive with a Torsionable Lead-Screw

As a result of previous work on improving the slow motion control performance for a servo drive with a static braking torque a modified control system structure that makes use of potentialities offered by controllers of the ACOPOS servo drive has been developed [2].

However, an additional corrective action needs to be introduced in view of the fact that the used lead-screw is torsionable. As a result of analysis made on such a servo drive a new structure of the servo drive has been developed (Fig. 10).

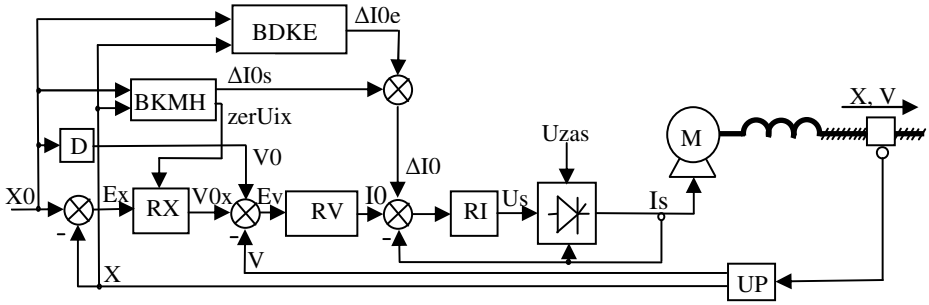

Fig. 10. Structure of the modified servo drive: BDKE – block for dynamic correction of the lead-screw torsionability, BKMH – block for correcting the effect produced by the static braking torque and resetting the integral action of the position controller (RX), zerUIx – signal resetting the integral action of the position controller; the remaining symbols as in Figs. 1–4

It includes two additional feedback paths. The one of them corrects effects that are attributable to the torsionability exhibited by the lead-screw. The nonlinear dynamic block (BDKE) in this feedback path corrects the auxiliary set-point (ΔI0) of the current controller (RI) of the servo drive on the basis of information about the rate of change of the machine tool slide position error in the vicinity of the desired slide position. The value of the corrective signal ΔI0e is determined every 100 μs, i.e. as frequent as the algorithm of the current controller (RI) is repeated.

The other feedback path with the corrective block (BKMH) generates a signal ΔI0s in order to minimize the effect of the braking torque at rest on the control performance during slow motions carried out by the servo drive and changes in the direction of the motion. The ΔI0s signal also adjusts the set-point of the current controller (RI). The way the signal is generated and its parameters are determined is described in [2]. Additionally, the BKMH block resets the integral action of the position controller (RX) in the case that the position error (X0-X) equals zero or changes its sign at the preset velocity being equal to zero. This provides a reduction in overshoots occurring during large changes in the set-point and a reduction in time the set-point is reached. The results of simulation tests indicate that the servo drive with a stiff lead-screw is controlled with very great accuracy over a wide range of its variations in load, and thereby variations in the associated static braking torque [2].

In using the BDKE block of the structure shown in Fig. 11 an empirical relationship between the gain Ke and the machine tool slide position X, which minimizes the overshoot during minimal stepwise changes in the desired slide position occurring in the process of micromachining, has been derived during the tests. The relationship is depicted in Fig. 12.

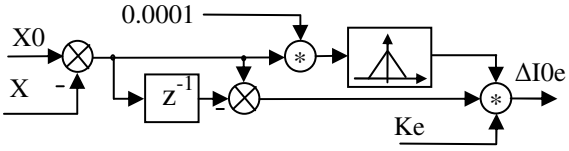

Fig. 11. Structure of the analytical block BDKE; K1, K2 and K3 - coefficients

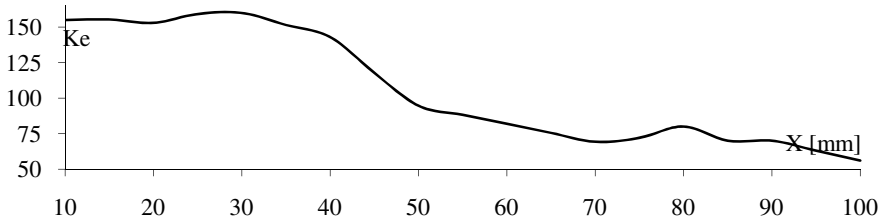

Fig. 12. Relationship between the Ke gain of the BDKE block and the slide position X, which provides a minimal overshoot during minimal stepwise changes in the slide position set-point

Considering the fact that the function Ke(X) is nonlinear, its fuzzy approximation has been determined, and in Fig. 13 the structure of the BDKE block making use of it is shown. The membership functions for its inputs X1 and X2 and output Ke are given in Fig. 14.

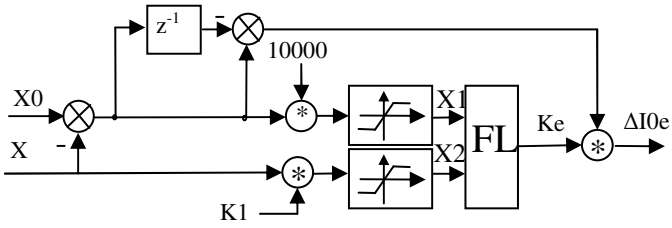

Fig. 13. Structure of the fuzzy block BDKE

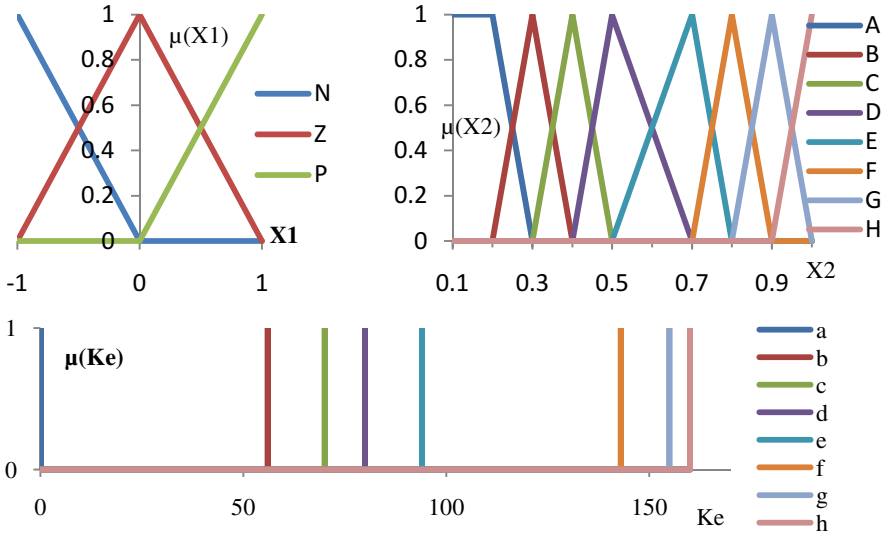

Fig. 14. Membership functions used in the fuzzy block BDKE

The fuzzy inference algorithm of the BDKE block makes use of the control law shown in Table 1 and logic operators defined by Zadeh and the MIN-MAX inference mechanism [7].

Table 1. Inference rules for the BDKE block.

X1 \ X2	A	B	C	D	E	F	G	H
N	a	a	a	a	a	a	a	a
Z	g	h	f	e	d	e	c	b
P	a	a	a	a	a	a	a	a

The result of inference is defuzzyfied by means of the height method. The K1 coefficient has been chosen so that the entire range of slide positions X be covered by the range of signal X2 variations.

5 Results of Simulation Tests

During the simulation tests the operational effectiveness of the presented servo drive with a fuzzy block to correct dynamically the lead-screw torsionability (BDKE) has been studied.

In Figures 15 and 16 there is shown the behavior of the slide position error (*Ex*) for several initial positions of the slide during the simulated servo drive motion after a stepwise change in its position set-point by 0.001 mm with and without the BDKE block. In Fig. 17 there is shown the value of the overshoot before and after the BDKE block has been employed for various slide positions X and a stepwise change in its position set-point by 0.001 mm.

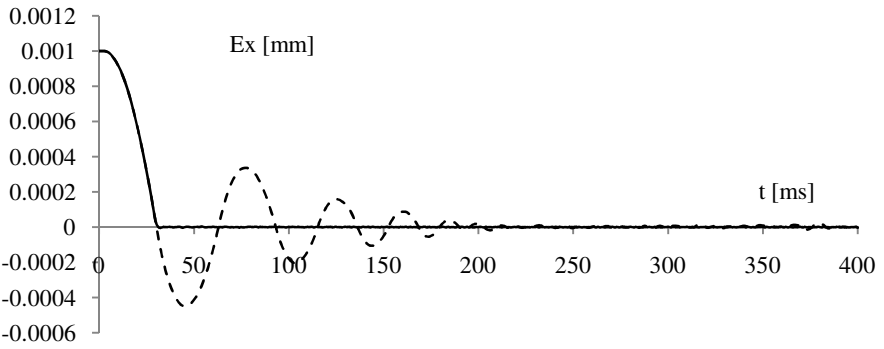

Fig. 15. Tracking errors during the first 400 ms after a stepwise change in the position set-point by X*0* = 0.001 mm from the initial value X=10 mm of the servo drive before (broken line) and after (solid line) the modification

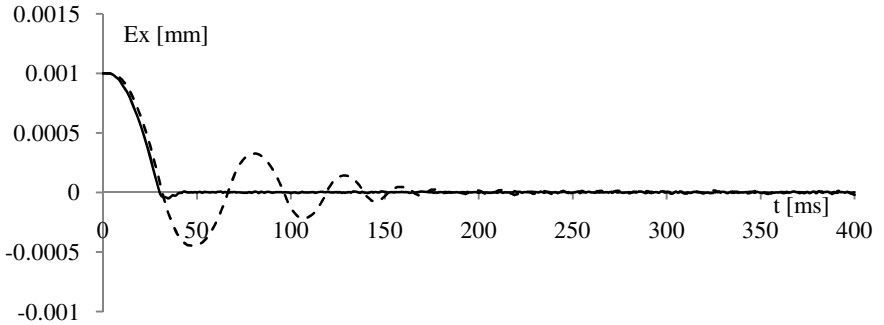

Fig. 16. Tracking errors during the first 400 ms after a stepwise change in the position set-point by X*0* = 0.001 mm from the initial value X=100 mm of the servo drive before (broken line) and after (solid line) the modification

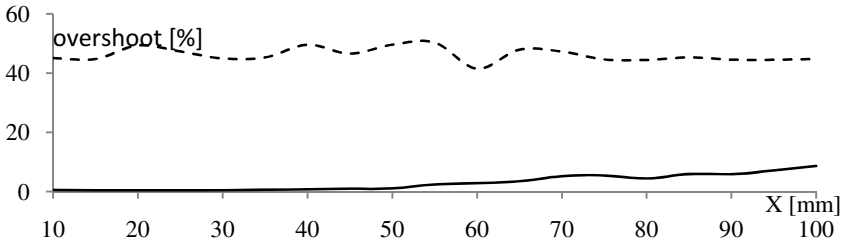

Fig. 17. Overshoots during a stepwise change in the position set-point by 0.001 mm of the servo drive before (broken line) and after the modification (solid line)

In Figs. 18 – 21 there is depicted the behavior of the slide position error during the simulated slide motion with a constant preset velocity of V0=0.001 mm/s for the servo drive with and without the BDKE block and various initial slide positions x. Owing to the use of the BDKE block the highest and the lowest values of the slide position error have decreased over fivefold for a short lead-screw and twofold for a long lead-screw.

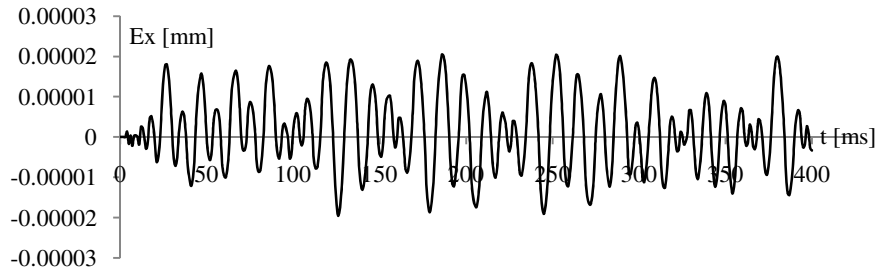

Fig. 18. Tracking error during the first 400 ms after a linear change in the position set-point by V*0* = 0.001 mm/s for the initial slide position X=10 mm – classic servo drive

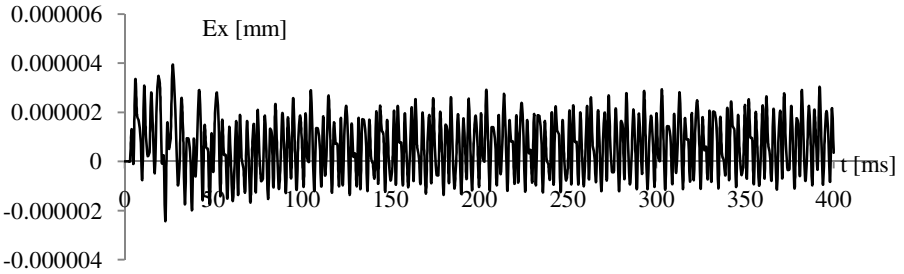

Fig. 19. Tracking error during the first 400 ms after a linear change in the position set-point by V*0* = 0.001 mm/s for the initial slide position X=10 mm – modified servo drive

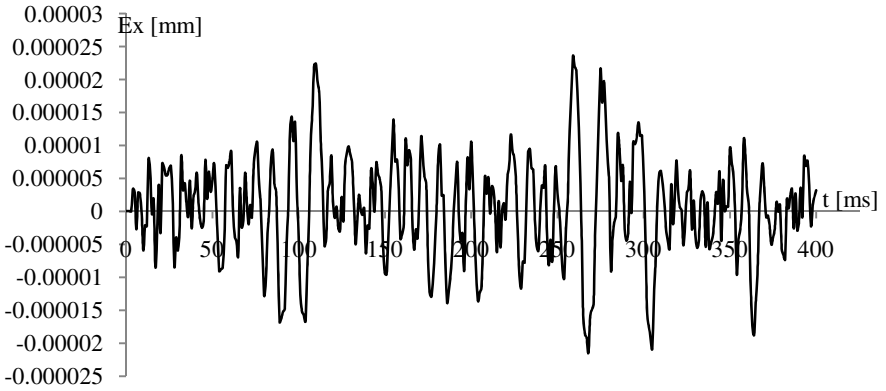

Fig. 20. Tracking error during the first 400 ms after a linear change in the position set-point by V*0* = 0.001 mm/s for the initial slide position X=100mm – classic servo drive

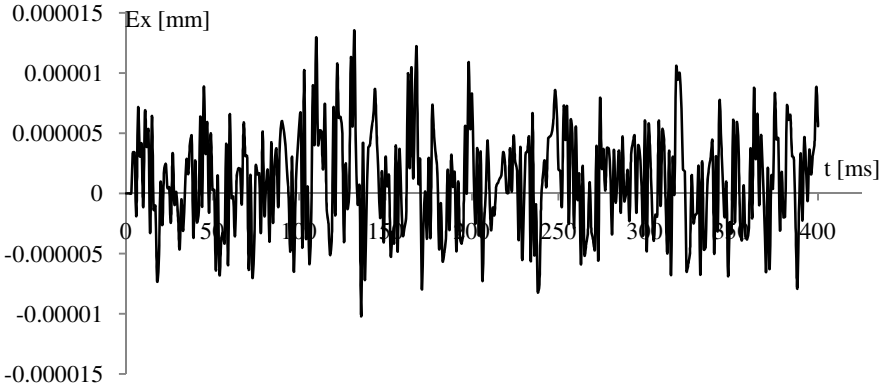

Fig. 21. Tracking error during the first 400 ms after a linear change in the position set-point by V*0* = 0.001 mm/s for the initial slide position X=100 mm – modified servo drive

All simulations have been carried out with controllers settings (RX, RV and RI) chosen to control the motion of a servo drive motor developing high velocities at no-load.

Comparison of simulation results obtained for the servo drive with a torsionable lead-screw and strong static friction before and after the fuzzy BDKE block has been employed shows that a significant improvement in slow motion control performance has been obtained. The fact that such high control accuracy has been achieved with controller settings chosen for high velocities developed by a servo drive at no-load makes the presented solution even more attractive.

6 Summary

In the paper a simple method for improving the motion control performance of a servo drive with a torsionable lead-screw and a degressive static friction at small reference velocities and small stepwise changes in the reference position is presented. The method consists in introducing an additional nonlinear feedback that adjusts the set-point of the current controller of the servo drive. The simulation tests provide evidence in support of effectiveness of the described algorithm, which also can be applied to digital servo drives of other types.

In the nearest future it is planned to perform practical tests to verify the effectiveness of the algorithm described.

Acknowledgments. This work has been founded by Polish National Science Centre under project N N504 643940

References

1. ACOPOS – Users manual, Bernecker & Rainer
2. Broel-Plater, B.: A method for performance of low-speed control designed for a digital servo drive. Przegląd Elektrotechniczny 88(10a), 74–79 (2012) (in polish)
3. Dornfeld, D., Lee, D.-E.: Precision Manufacturing. Springer, Heidelberg (2008)
4. Kamiński, M., Orłowska-Kowalska, T.: Application of Radial Basic Funktion Neural Networki in speed control of the driver with elastic connection. SENE (2013)
5. Krishnan, R.: Motor Drives – Modeling, analysis and Control. Prentice Hall (2001)
6. Makkapati, V.P., Reinchhartinger, M., Horn, M.: Performed Improvement of a Servo Drives with Mechanical Elasticity via Extended Acceleration Feedback. In: IEEE Intern. Conf. on Control Application, Dubrownik, pp. 1279–1284 (2012)
7. Rutkowski, L.: Computational Intelligence. Methods and Techniques. Springer, Heidelberg (2008)
8. Sato, K., Nakamoto, K., Shimokohbe, A.: Practical control of precision positioning with friction. Precision Engineering 28, 426–434 (2004)
9. Suh, S.-H., Kang, S.-K., et al.: Theory and Design of CMC Systems. Springer, Heidelberg (2003)
10. Sato, K., Nakamoto, K., Shimokohbe, A.: Practical control of precision positioning with friction. Precision Engineering 28, 426–434 (2004)

Chaos Synchronization of the Modified Van der Pol-Duffing Oscillator of Fractional Order

Mikołaj Busłowicz[1] and Adam Makarewicz[2]

[1] Białystok University of Technology, Faculty of Electrical Engineering
busmiko@pb.edu.pl
[2] Doctoral Study, Faculty of Electrical Engineering, Białystok University of Technology
adammakarewicz@interia.pl

Abstract. The paper considers the modified Van der Pol-Duffing oscillator of fractional order. Chaotic behavior of the system is analyzed and the problem of synchronization of two modified Van der Pol-Duffing systems via master/slave configuration with linear coupling is considered. A simple sufficient condition for synchronization is proposed. This condition is based on the chaos stabilization method derived by Jiang et. al. [Chaos Solitons and Fractals, 2003] for the global synchronization of two coupled general chaotic integer order systems with a unidirectional linear error feedback coupling. Numerical simulations show the effectiveness of theoretical considerations.

Keywords: fractional, Van der Pol-Duffing system, chaos, synchronization.

1 Introduction

Dynamical systems described by fractional order differential or difference equations have been investigated in several areas such as viscoelasticity, electrochemistry, diffusion processes, control theory, electrical engineering, etc. The problems of analysis and synthesis of dynamic systems described by fractional order differential (or difference) equations recently have considerable attention, see monographs [8, 13, 15–18], for example.

Many non-linear dynamical systems have behavior known as chaos. Chaos is a very interesting non-linear phenomenon. Synchronization of chaos is a very interesting problem, enjoying a wide interest, for example, in control technology, cryptography, communications [9, 19], etc. The problem of synchronization of chaos recently has been intensively studied in many papers, see for example [3, 4, 7, 10, 11, 24] for systems of integer order and [2, 6, 12, 14, 16, 20, 21] for system of fractional order.

In this paper we consider the modified Van der Pol-Duffing oscillator of fractional order. Chaotic behavior of this system will be analyzed and simple sufficient condition for synchronization of two such systems with non-commensurate fractional orders via master/slave configuration with linear coupling will be given. The proposed condition for synchronization is based on the chaos synchronization method derived in [7] in the case of integer order systems (see also [3]). The method given in

R. Szewczyk, C. Zieliński, and M. Kaliczyńska (eds.), *Recent Advances in Automation, Robotics and Measuring Techniques*, Advances in Intelligent Systems and Computing 267,
DOI: 10.1007/978-3-319-05353-0_4,

[7] was applied in [12] to chaos synchronization in modified Van der Pol-Duffing system of fractional commensurate order.

2 Preliminaries

The modified Van der Pol-Duffing oscillator is described by following normalized non-linear differential equation

$$\dot{X}(t) = f(X(t)) = \begin{bmatrix} -m[x^3(t) - \mu x(t) - y(t)] \\ x(t) - y(t) - z(t) \\ \beta y(t) \end{bmatrix}, \quad X(t) = \begin{bmatrix} x(t) \\ y(t) \\ z(t) \end{bmatrix}. \tag{1}$$

The oscillator (1) recently was considered in [24] (integer order) and [12] (fractional order) for various values of parameters. We consider the following parameters

$$m = 100, \ \mu = 0.2 \ \text{ and } \ \beta = 300. \tag{2}$$

For these parameters the system (1) exhibits a double-scroll chaotic attractor, as shown in Fig. 1 (for initial conditions $x(0) = z(0) = 0.05$ and $y(0) = 0$). Trajectories of the system were obtained using Simulink package of MATLAB.

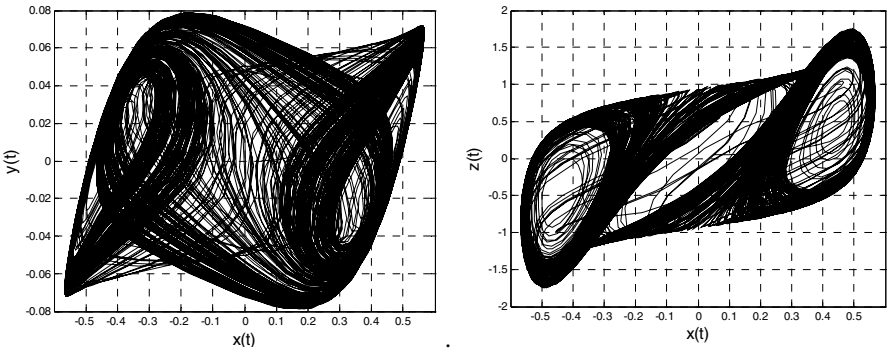

Fig. 1. Chaotic trajectory of the system (1)

In this paper we consider the modified Van der Pol-Duffing oscillator of fractional non-commensurate order, described by the state equation

$$D_t^{\overline{\alpha}} X(t) = f(X(t)) = \begin{bmatrix} -m[x^3(t) - \mu x(t) - y(t)] \\ x(t) - y(t) - z(t) \\ \beta y(t) \end{bmatrix}, \quad D_t^{\overline{\alpha}} X(t) = \begin{bmatrix} D_t^{\alpha_1} x(t) \\ D_t^{\alpha_2} y(t) \\ D_t^{\alpha_3} z(t) \end{bmatrix}, \tag{3}$$

with parameters (2), where derivatives of fractional orders satisfy the inequality $0<\alpha_i<1$ for $i=1,2,3$,

$$D_t^{\alpha_i}x(t)=\frac{1}{\Gamma(1-\alpha_i)}\int_0^t\frac{x'(\tau)\mathrm{d}\tau}{(t-\tau)^{\alpha_i}},\ 0<\alpha_i<1, \tag{4}$$

is the Caputo definition for derivative of fractional order α_i, where $x'(t)=dx(t)/dt$ and $\Gamma(\alpha_i)=\int_0^\infty e^{-t}t^{\alpha_i-1}dt$ is the Euler gamma function.

3 Stability Analysis

The fractional order system (3) (similarly as the natural order system (1)) has three equilibrium points. These point are obtained by solution of the non-linear equation $f(X(t))=0$, i.e. the set of equations

$$0=-m[x^3(t)-\mu x(t)-y(t)],\ \ 0=x(t)-y(t)-z(t),\ \ 0=\beta y(t). \tag{5}$$

Solving the equations (5) for parameters (2) one obtains the following equilibrium points

$$E_0=\begin{bmatrix}0\\0\\0\end{bmatrix},\ \ E_1=\begin{bmatrix}\sqrt{\mu}\\0\\\sqrt{\mu}\end{bmatrix}=\begin{bmatrix}\sqrt{2}\\0\\\sqrt{2}\end{bmatrix},\ \ E_2=\begin{bmatrix}-\sqrt{\mu}\\0\\-\sqrt{\mu}\end{bmatrix}=\begin{bmatrix}-\sqrt{2}\\0\\-\sqrt{2}\end{bmatrix}. \tag{6}$$

Let

$$A_k=\left.\frac{\partial f(X)}{\partial X}\right|_{X=E_k}=\left.\begin{bmatrix}-m(3x^2(t)-\mu) & m & 0\\ 1 & -1 & -1\\ 0 & \beta & 0\end{bmatrix}\right|_{X=E_k},\ k=0,1,2, \tag{7}$$

be the Jacobian matrix of the function $f(X)$ evaluated at $X=E_k$ ($k=0,1,2$).

First we assume that fractional orders of the system satisfy the condition $\alpha_1=\alpha_2=\alpha_3=\alpha$. In this case the linearized system (3) about its the equilibrium point E_k ($k=0,1,2$) has the form

$$D_t^{\alpha}X(t)=A_kX(t), \tag{8}$$

where the matrix A_k is computed form (7) for parameters (2).

It is well known [1] that the fractional order system (8) is stable if and only if its characteristic polynomial of fractional degree has no zeros in the closed right-half of the Riemann complex surface, i.e.

$$w(s) = \det(s^{\alpha} I - A) \neq 0 \text{ for } \operatorname{Re} s \geq 0, \tag{9}$$

or equivalently, the following condition is satisfied

$$|\arg \lambda_i(A)| > \alpha\pi/2, \quad i = 1,2,...,n, \tag{10}$$

where $\lambda_i(A)$ is the i-th eigenvalues of matrix A.
The condition (10) can be written in the form

$$\alpha < 2\phi/\pi, \quad \phi = \min_i |\arg \lambda_i(A)|. \tag{11}$$

Now, we check the stability of the equilibrium points (6). From (7) we have

$$A_0 = \begin{bmatrix} m\mu & m & 0 \\ 1 & -1 & -1 \\ 0 & \beta & 0 \end{bmatrix} = \begin{bmatrix} 20 & 100 & 0 \\ 1 & -1 & -1 \\ 0 & 300 & 0 \end{bmatrix}, \tag{12}$$

$$A_1 = A_2 = \begin{bmatrix} -2m\mu & m & 0 \\ 1 & -1 & -1 \\ 0 & \beta & 0 \end{bmatrix} = \begin{bmatrix} -40 & 100 & 0 \\ 1 & -1 & -1 \\ 0 & 300 & 0 \end{bmatrix}. \tag{13}$$

Computing eigenvalues of matrices (12), (13) one obtains

- for A_0: $\lambda_1 = 22.7086;\ \lambda_{2,3} = -1.8543 \pm j16.1486$,
- for $A_2 = A_3$: $\lambda_1 = -42.0745;\ \lambda_{2,3} = 0.5372 \pm j16.8796$.

The matrix A_0 has real positive eigenvalue which lies in instability region. This means that the equilibrium point E_0 is unstable for all $\alpha \in (0,1)$.

The matrices $A_2 = A_3$ have two eigenvalues with positive real pats. From (11) it follows that the equilibrium points E_1 and E_2 are locally stable for

$$\alpha < \frac{2}{\pi} \arctan \frac{16.8796}{0.5372} = 0.9797. \tag{14}$$

From the above it follows that the system (8) has a chaotic behavior for $\alpha > 0.98$.

Using numerical simulations for $\alpha = 0.985$, $\alpha = 0.98$, $\alpha = 0.9795$ and $\alpha = 0.97$ one obtains the plots shown in Fig. 2. When $\alpha = 0.985$ double-band chaotic behavior is observed. For $\alpha = 0.98$ the system is chaotic with one-band chaos. For $\alpha = 0.9795$ the limit cycle is found and when $\alpha = 0.97$ asymptotically stable attractor exists. Trajectories of the system for $\alpha = 1$ are shown in Fig. 1.

Simulations were performed using the Ninteger Fractional Control Toolbox for MatLab [22]. In this toolbox exists a Simulink block *nid* for fractional derivative and integral. Order and method for rational approximation of fractional derivative/integral can be selected. In simulations we select the Oustaloup's approximation technique (CRONE) of order *n*=7. The block *nid* has the transfer function ks^{v}, where v is real a number from the interval $(-1,1)$. In simulations the fractional integrator $1/s^{\alpha}$ is modeled by series connection of the classical integrator and the block *nid.* Transfer function of this connection is k/s^{v-1}. It is easy to see that $v \in (0,1)$ for $\alpha \in (0,1)$.

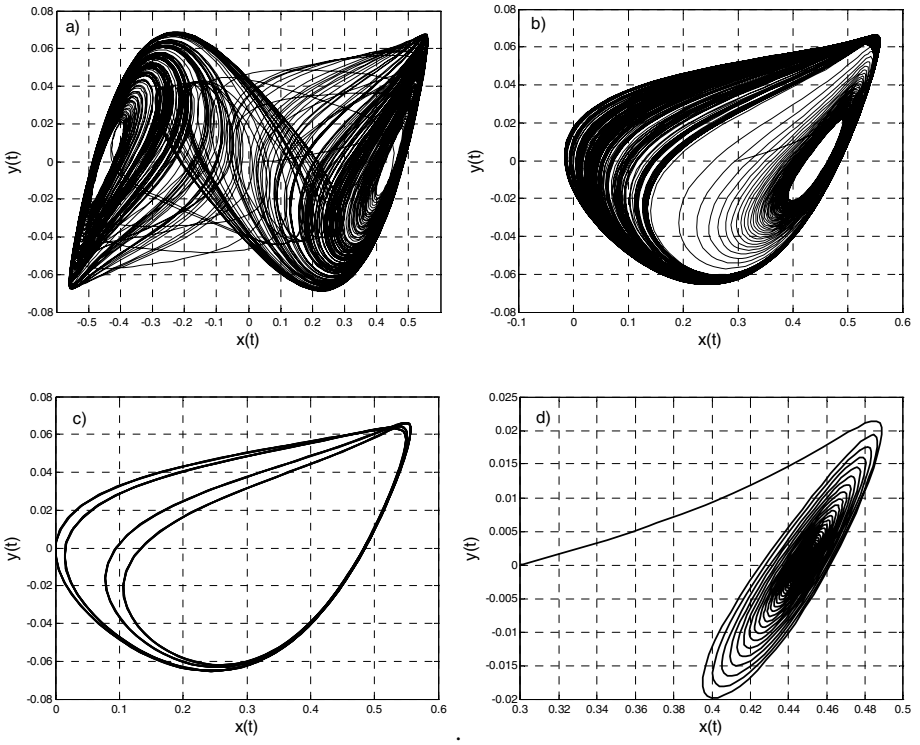

Fig. 2. Trajectories of the system (8): a) α=0.985; b) α=0.98; c) α=0.9795; d) α=0.97

Now, using numerical simulations we investigate chaotic behavior of the system (3) with non-commensurate fractional orders and we obtain that the system is chaotic for $\alpha_1 = 0.82$ and $\alpha_2 = \alpha_3 = 0.98$. Chaotic trajectories are shown in Fig. 3.

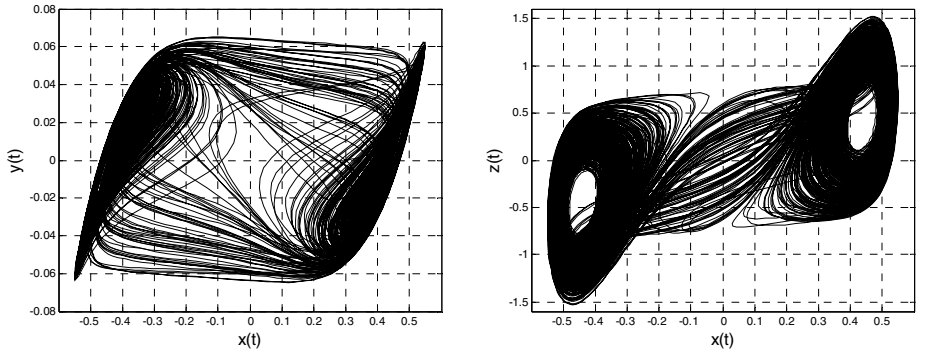

Fig. 3. Chaotic trajectories of the system (3) for α_1=0.82 and α_2=α_3=0.98

4 Synchronization

Let the fractional system (3) with $\alpha_1 = 0.82$ and $\alpha_2 = \alpha_3 = 0.98$ be the Master system and the coupled Slave fractional-order system is described by

$$D_t^{\overline{\alpha}} \overline{X}(t) = \begin{bmatrix} -m[\overline{x}^3(t) - \mu\overline{x}(t) - \overline{y}(t)] \\ \overline{x}(t) - \overline{y}(t) - \overline{z}(t) \\ \beta\overline{y}(t) \end{bmatrix} + KE(t), \quad D_t^{\overline{\alpha}} \overline{X}(t) = \begin{bmatrix} D_t^{\alpha_1}\overline{x}(t) \\ D_t^{\alpha_2}\overline{y}(t) \\ D_t^{\alpha_3}\overline{z}(t) \end{bmatrix}, \tag{15}$$

where $K = \mathrm{diag}(k_1, k_2, k_3)$, $k_i \geq 0$, and

$$E(t) = \begin{bmatrix} e_x(t) \\ e_y(t) \\ e_z(t) \end{bmatrix} = X(t) - \overline{X}(t) = \begin{bmatrix} x(t) - \overline{x}(t) \\ y(t) - \overline{y}(t) \\ z(t) - \overline{z}(t) \end{bmatrix} \tag{16}$$

is the synchronization error.

We select a feedback gain K such that $\lim_{t\to\infty} \|E(t)\| = 0$, where $\|.\|$ denotes the Euclidean norm.

Using (3) and (15), the error dynamics of coupled systems can be written in the form

$$D_t^{\overline{\alpha}} E(t) = \begin{bmatrix} -m[({x_1}^3(t) - {\overline{x}_1}^3(t)) - \mu e_x(t) - e_y(t)] \\ e_x(t) - e_y(t) - e_z(t) \\ \beta e_y(t) \end{bmatrix} - KE(t). \tag{17}$$

Using the relation

$$x^3(t) - \overline{x}^3(t) = [x(t) - \overline{x}(t)][x^2(t) + x(t)\overline{x}(t) + \overline{x}^2(t)] = e_x(t)k_x, \tag{18}$$

where

$$k_x = x^2(t) + x(t)\bar{x}(t) + \bar{x}^2(t), \tag{19}$$

the equation (17) can be written in the form

$$D_t^{\bar{\alpha}} E(t) = (A - K + M_x)E(t), \tag{20}$$

with

$$A = \begin{bmatrix} m\mu & m & 0 \\ 1 & -1 & -1 \\ 0 & \beta & 0 \end{bmatrix}, \quad M_x = \begin{bmatrix} -mk_x & 0 & 0 \\ 0 & 0 & 0 \\ 0 & 0 & 0 \end{bmatrix}. \tag{21}$$

To select a feedback gain matrix K, we apply the method proposed in [7] (see also [3]) for stabilization of chaos in integer order systems. This method has been applied in [12] to the modified Van der Pol-Duffing system with fractional commensurate order. The method of [7] gives the sufficient condition for stability of coupled natural order chaotic systems. In this method the time-dependent parameter (19) is treated as a interval parameter which values belong to known interval with known bounds, i.e. $k_x \in [a, b]$, where a and b are known.

The system under consideration is a chaotic system with bounded values of state variables. From Fig. 3 it follows that $x(t) \in [-0.06, 0.06]$ and (since the Slave system has the same dynamic as Master) $\bar{x}(t) \in [-0.06, 0.06]$. Hence, form (19) we have that $k_x \in [0, 0.0108]$ for all $t > 0$.

Similarly as in [12], we consider the case of integer order system (20), i.e. the system (20) with $\alpha_1 = \alpha_2 = \alpha_3 = 1$. In this case the equation (21) takes the form

$$\dot{E}(t) = (A - K + M_x)E(t). \tag{22}$$

To select a feedback gain matrix K, we apply the Lyapunov stability theory to the system (22).

Let

$$V(t) = E^{\mathrm{T}}(t)PE(t), \tag{23}$$

where P is a positive definite symmetric constant matrix, be the Lyapunov function for the system (22).

The derivative of (23) along solution of (22) is as follows

$$\dot{V}(t) = \dot{E}^{\mathrm{T}}(t)PE(t) + E^{\mathrm{T}}(t)P\dot{E}(t) = E^{\mathrm{T}}(t)[A_c{}^{\mathrm{T}}P + PA_c]E(t), \tag{24}$$

where $A_c = A - K + M_x$.

The equation (24) can be written in the form

$$\dot{V}(t) = E^{\mathrm{T}}(t)QE(t), \tag{25}$$

where

$$Q = A_c{}^{\mathrm{T}}P + PA_c = (A^{\mathrm{T}} - K^{\mathrm{T}} + M_x{}^{\mathrm{T}})P + P(A - K + M_x). \tag{26}$$

According to the Lyapunov stability theory, the system (22) is asymptotically stable if and only if $\dot{V}(t) < 0$ for $t \geq 0$, or equivalently, the symmetric matrix Q defined by (26) is negative definite (all eigenvalues have negative real parts).

To check when the matrix (26) has all eigenvalues with negative real parts, we apply the Gershgorin theorem [5, 23].

From (21) it follows that the matrix Q defined by (26) has the following form

$$Q = \begin{bmatrix} m\mu - k_1 - mk_x & 1 & 0 \\ m & -1-k_2 & \beta \\ 0 & -1 & -k_3 \end{bmatrix} P + P \begin{bmatrix} m\mu - k_1 - mk_x & m & 0 \\ 1 & -1-k_2 & -1 \\ 0 & \beta & -k_3 \end{bmatrix}. \tag{27}$$

If we choose $P = \mathrm{diag}(p_1, p_2, p_3)$ with $p_i = 1 > 0$, then we obtain

$$Q = \begin{bmatrix} 2(m\mu - k_1 - mk_x) & m+1 & 0 \\ m+1 & -2(1+k_2) & \beta - 1 \\ 0 & \beta - 1 & -2k_3 \end{bmatrix}. \tag{28}$$

From the Gershgorin theorem we have that all eigenvalues of (28) have negative real parts if the following conditions are satisfied

$$2(m\mu - k_1 - mk_x) + m + 1 < 0,$$

$$-2(1+k_2) + m + 1 + |\beta - 1| < 0,$$

$$-2k_3 + |\beta - 1| < 0.$$

Since $k_x \in [0, 0.0108]$, from the above and (2) we obtain

$$k_1 > 0.5(2m\mu - 2mk_x + m + 1) = 69.42,$$

$$k_2 > 0.5(-2 + 101 + 299) = 199,$$

$$k_3 > 299/2 = 149.5.$$

This means that we can chose $k_1 = 71,\ k_2 = 200,\ k_3 = 150$. For these values of gain matrix $K = \mathrm{diag}(k_1, k_2, k_3)$ the system (22) is asymptotically stable. To check stability of the fractional order system (20), we perform numerical simulations.

Using numerical simulations for $\alpha_1 = 0.82$ and $\alpha_2 = \alpha_3 = 0.98$ we investigate the synchronization problem of two coupled chaotic the modified Van der Pol-Duffing systems (3), (15) for $k_1 = 71,\ k_2 = 200,\ k_3 = 150$ and for lesser feedback gain coefficients. From simulations we obtain that synchronization holds for $k_1 = 71,\ k_2 = 200,\ k_3 = 150$ and also for values of these coefficients essentially smaller, for example, for $k_1 = 12$ and $k_2 = k_3 = 10$. Results of simulations are shown in Fig. 4 with initial conditions for the system (3): $x(0) = z(0) = 0.05,\ y(0) = 0$ and for the system (15): $\bar{x}(0) = 0.5,\ \bar{y}(0) = -0.2,\ \bar{z}(0) = -0.5$. From this figure it follows that synchronization is attained at about 0.1 second for $k_1 = 71,\ k_2 = 200,\ k_3 = 150$ and at about 0.6 second for $k_1 = 12$ and $k_2 = k_3 = 10$.

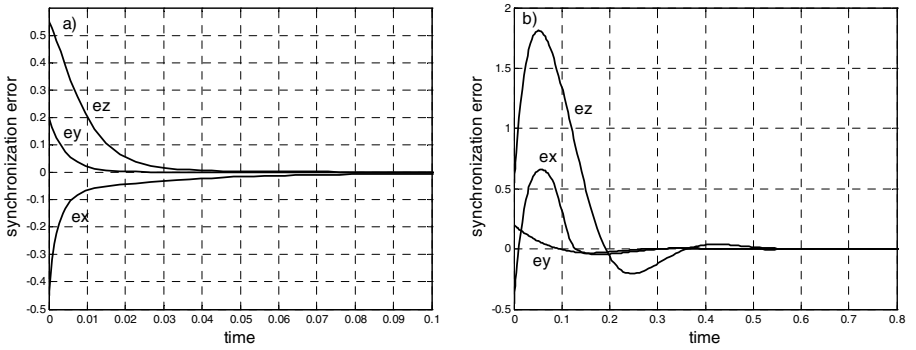

Fig. 4. Synchronization error: a) for k_1=71, k_2=200, k_3=150; b) for k_1=12, k_2=k_3=10

5 Concluding Remarks

Chaotic behavior of the modified Van der Pol-Duffing oscillator of fractional order has been analyzed and the problem of synchronization of two such systems with linear coupling has been considered. A simple necessary condition for chaotic behavior of the system with commensurate orders of derivatives and a simple sufficient condition for synchronization of two coupled systems with non-commensurate orders have been proposed. Numerical simulations showed the effectiveness of theoretical considerations.

Acknowledgement. The work was supported by the National Science Center in Poland under grant N N514 638940.

References

1. Busłowicz, M.: Stability of State-Space Models of Linear Continuous-time Fractional Order Systems. Acta Mechanica et Automatica 5, 15–22 (2011)
2. Busłowicz, M., Makarewicz, A.: Synchronization of the Chaotic Ikeda Systems of Fractional Order. In: Mitkowski, W., Kacprzyk, J., Baranowski, J. (eds.) Theory & Appl. of Non-integer Order Syst. LNEE, vol. 257, pp. 261–269. Springer, Heidelberg (2013)
3. Deleanu, D.: On a Sufficient Criterion for Global Synchronization in Chaotic Systems. In: Kanarachos, A. (ed.) Recent Advances in Telecommunications, Signals and Systems, pp. 95–100. WSEAS Press (2013)
4. Dibakar, G.A., Chowdhury, R., Saha, P.: On the Various Kinds of Synchronization in Delayed Duffing-Van der Pol System. Commun. Nonlinear Sci. Numer. Simulat. 13, 790–803 (2008)
5. Gantmacher, F.R.: The Theory of Matrices. Nauka, Moscow (1966) (in Russian)
6. He, G.T., Luo, M.: Dynamic Behavior of Fractional Order Duffing Chaotic System and its Synchronization via Singly Active Control. Appl. Math. Mech. 33(5), 567–582 (2012)
7. Jiang, G.-P., Tang, W.K.-S., Chen, G.: A Simple Global Synchronization criterion for Coupled Chaotic Systems. Chaos Solitons and Fractals 15, 925–935 (2003)
8. Kaczorek, T.: Selected Problems of Fractional Systems Theory. LNCIS, vol. 411. Springer, Heidelberg (2011)
9. Kenfack, G., Tiedeu, A.: Secured Transmission of ECG Signals: Numerical and Electronic Simulations. Journal of Signal and Information Processing 4, 158–169 (2013)
10. Kimiaeifar, A., Saidi, A.R., Sohouli, A.R., Ganji, D.D.: Analysis of Modified Van der Pol's Oscillator Using He's Parameter-Expanding Methods. Current Applied Physics 10, 279–283 (2010)
11. Mahmoud, G.M., Aly, S.A., Farghaly, A.A.: On Chaos Synchronization of a Complex Two Coupled Dynamos System. Chaos, Solitons and Fractals 33, 178–187 (2007)
12. Matouk, A.E.: Chaos, Feedback Control and Synchronization of a Fractional-Order Modified Autonomous Van der Pol–Duffing Circuit. Commun. Nonlinear Sci. Numer. Simulat. 16, 975–986 (2011)
13. Monje, C., Chen, Y., Vinagre, B., Xue, D., Feliu, V.: Fractional-Order Systems and Controls. Springer, London (2010)
14. Menacer, T., Hamri, N.: Synchronization of Different Chaotic Fractional-Order Systems via Approached Auxiliary System the Modified Chua Oscillator and the Modified Van der Pol-Duffing Oscillator. Electronic Journal of Theoretical Physics, EJTP 8(25), 253–266 (2011)
15. Ostalczyk, P.: Epitome of the Fractional Calculus, Theory and its Applications in Automatics. Publishing Department of Technical University of Łódź, Łódź (2008) (in Polish)
16. Petras, I.: Fractional-Order Nonlinear Systems Modeling, Analysis and Simulation. Higher Education Press, Springer, Beijing, Heidelberg (2011)
17. Podlubny, I.: Fractional Differential Equations. Academic Press, San Diego (1999)
18. Sabatier, J., Agrawal, O.P., Machado, J.A.T. (eds.): Advances in Fractional Calculus, Theoretical Developments and Applications in Physics and Engineering. Springer, London (2007)
19. Sheu, L.J., Chen, W.C., Chen, Y.C., Wenig, W.T.: A Two-Channel Secure Communication Using Fractional Chaotic Systems. World Academy of Science, Engineering and Technology 65, 1057–1061 (2010)

20. Suchorsky, -M.K., Rand, R.H.: A Pair of Van der Pol Oscillators Coupled by Fractional Derivatives. Nonlinear Dyn. 69, 313–324 (2012)
21. Wang, Y., Yin, X., Liu, Y.: Control Chaos in System with Fractional Order. Journal of Modern Physics 3, 496–501 (2012)
22. Valério, D.: Ninteger v. 2.3 - Fractional Control Toolbox for MatLab, User and Programmer Manual, Technical University of Lisbona, Lisbona (2005), http://web.ist.utl.pt/duarte.valerio/ninteger/ninteger.htm
23. Varga, R.S.: Gershgorin and His Circles. Springer, Berlin (2004)
24. Vincent, U.E., Odunaike, R.K., Laoye, J.A., Gbindinninuola, A.A.: Adaptive Backstepping Control and Synchronization of a Modified and Chaotic Van der Pol-Duffing Oscillator. J. Control Theory Appl. 9(2), 273–277 (2011)

Stability Analysis of Descriptor Continuous-Time Two-Term Linear Systems of Fractional Orders

Mikołaj Busłowicz

Białystok University of Technology, Faculty of Electrical Engineering, Białystok, Poland
busmiko@pb.edu.pl

Abstract. The stability problem of fractional continuous-time descriptor linear systems described by the state equation with two differential operators of fractional orders has been considered. Such systems are called the two-term systems. The analytic and frequency domain methods for stability checking of the system with commensurate orders of fractional derivatives have been given. The frequency domain method is based on the Argument Principle and it is simple to apply. The considerations are illustrated by numerical example.

Keywords: linear system, descriptor, continuous-time, fractional, stability.

1 Introduction

In the last decades, the problem of analysis and synthesis of dynamic systems described by fractional order differential or difference equations has been considered in many books (see [9, 15, 18, 20, 21], for example, and references therein).

The problem of stability of linear fractional order systems has been investigated in monographs mentioned above and in the papers [1, 3, 4, 14, 19, 22, 23] for continuous-time systems and in [2, 5, 7, 8, 12] for discrete-time systems.

Recently, the stability problem of the fractional-order systems with double fractional orders has been considered in [6] and [13]. Such systems are also called the two-term systems as a special case of multi-term systems [9].

The state of the art in the descriptor systems theory in given in [10]. The problem of stability of positive descriptor linear systems recently has been addressed in [16].

The aim of the paper is to give the analytic and the frequency domain method for stability analysis of descriptor continuous-time state-space two-term linear systems of fractional commensurate orders.

2 Problem Formulation

Consider a continuous-time two-term descriptor linear system of fractional orders described by the homogeneous state equation

$$E D_t^{k_2\alpha} x(t) + A_1 D_t^{k_1\alpha} x(t) = Ax(t), \quad 0 < \alpha \le 1, \tag{1}$$

R. Szewczyk, C. Zieliński, and M. Kaliczyńska (eds.), *Recent Advances in Automation, Robotics and Measuring Techniques*, Advances in Intelligent Systems and Computing 267,
DOI: 10.1007/978-3-319-05353-0_5,

where positive numbers k_1 and k_2 satisfy the inequality $k_2 > k_1$, $x(t) \in R^n$ is the state vector and $E, A, A_1 \in R^{n \times n}$ are real matrices.

We will assume that

$$\text{rank } E = n_e < n \tag{2}$$

and

$$\text{rank } H(s) = n \text{ for some } s \in \boldsymbol{C}, \tag{3}$$

where $\boldsymbol{C}$ denotes the field of complex numbers and

$$H(s) = s^{k_2 \alpha} E + s^{k_1 \alpha} A_1 - A \tag{4}$$

is the characteristic matrix of the system.

In (1) the Caputo definition of the derivative of fractional order $0 < \alpha \leq 1$ has been used

$$D_t^{\alpha} x(t) = \frac{1}{\Gamma(1-\alpha)} \int_0^t \frac{x'(\tau) d\tau}{(t-\tau)^{\alpha}}, \quad k = 1,2, \tag{5}$$

where $x'(t) = dx(t)/dt$ and $\Gamma(\alpha) = \int_0^{\infty} e^{-t} t^{\alpha-1} dt$ is the Euler gamma function.

In special case $\alpha = 1$ and $k_2 = 2$, $k_1 = 1$ the equation (1) describes the descriptor second-order dynamical system considered in [11].

The descriptor linear system (1) will be called stable if for any initial conditions $x(0) = x_0$ the solution $x(t)$ of the state equation (1) satisfies the condition

$$\lim_{t \to \infty} \left\| x(t) \right\| = 0. \tag{6}$$

It is well known that if the fractional order system is stable then norm of the state vector vanishes not exponentially but polynomially [22], i.e. there exist positive constants δ and β such that $\left\| x(t) \right\| \leq \delta t^{-\beta} \left\| x(0) \right\|$ for $t \geq 0$, where $\left\| \cdot \right\|$ denotes the norm.

The stability problem of the standard (i.e. with non-singular matrix E) system (1) has been recently considered in the papers [6, 13]. In these papers have been given the algebraic and frequency domain conditions for stability of the fractional system, described by more general state equation, of the form

$$D_t^{\alpha_2} x(t) + A_1 D_t^{\alpha_1} x(t) = Ax(t) + Bu(t), \tag{7}$$

where $0 < \alpha_1 < \alpha_2 \leq 1$.

The aim of the paper to give the analytic and frequency domain conditions for stability of the descriptor fractional order system (1).

3 The Main Results

For the new state-vector

$$\tilde{x}(t) = \begin{bmatrix} x(t) \\ D_t^{\alpha} x(t) \\ \vdots \\ D_t^{(k_2-1)\alpha} x(t) \end{bmatrix} \in R^{k_2 n} \tag{8}$$

the equation (1) can rewritten in the equivalent form

$$\tilde{E}\, D_t^{\alpha} \tilde{x}(t) = \tilde{A}\tilde{x}(t), \tag{9}$$

where

$$\tilde{E} = \begin{bmatrix} I_{(k_2-1)n} & \tilde{0}^{\mathrm{T}} \\ \tilde{0} & E \end{bmatrix} \in R^{k_2 n \times k_2 n}, \quad \tilde{A} = \begin{bmatrix} \tilde{0}^{\mathrm{T}} & I_{(k_2-1)n} \\ A & \tilde{A}_1 \end{bmatrix} \in R^{k_2 n \times k_2 n}, \tag{10}$$

$\tilde{0} \in \Re^{n \times (k_2-1)n}$ is the zero matrix, $()^{\mathrm{T}}$ denotes the transposition, $I_{(k_2-1)n}$ is the identity matrix and the block matrix $\tilde{A}_1$ of size $n \times (k_2 - 1)n$ has k_1-*th* block equal to $-A_1$ and remaining blocks are equal to zero.

If, $k_2 = 4$ and $k_1 = 2$, for example, then

$$\tilde{E} = \begin{bmatrix} I_n & 0_n & 0_n & 0_n \\ 0_n & I_n & 0_n & 0_n \\ 0_n & 0_n & I_n & 0_n \\ 0_n & 0_n & 0_n & E \end{bmatrix}, \quad \tilde{A} = \begin{bmatrix} 0_n & I_n & 0_n & 0_n \\ 0_n & 0_n & I_n & 0_n \\ 0_n & 0_n & 0_n & I_n \\ A & 0_n & -A_1 & 0_n \end{bmatrix}, \tag{11}$$

where 0_n is $n \times n$ the zero matrix and I_n is $n \times n$ the identity matrix.

From (10) and (2) it follows that

$$\tilde{n}_e = \operatorname{rank} \tilde{E} = (k_2 - 1)n + n_e < k_2 n. \tag{12}$$

Similarly as in [11] we introduce the following definition.

Definition 1. The fractional two-term descriptor system (1) will be called regular if the corresponding one-term descriptor system (9) is regular.

Lemma 1. The fractional two-term descriptor linear system (1) is regular if and only if there exists $s \in \boldsymbol{C}$ such that $w(s) \neq 0$, where

$$w(s) = \det H(s) = \det(s^{k_2\alpha} E + s^{k_1\alpha} A_1 - A). \tag{13}$$

Proof. It is well known that the fractional system (9) is regular if and only if [17]

$$\det(s^{\alpha}\tilde{E}-\tilde{A})\neq 0 \tag{14}$$

for some $s\in \boldsymbol{C}$, where the matrices $\tilde{E}$ and $\tilde{A}$ are defined in (10).

For simplicity of considerations we assume that $k_2=4$ and $k_1=2$. In this case the matrices $\tilde{E}$ and $\tilde{A}$ have the forms given in (11). Applying the elementary row and column operations to the matrix $s^{\alpha}\tilde{E}-\tilde{A}$ one obtains

$$s^{\alpha}\tilde{E}-\tilde{A}=\begin{bmatrix} s^{\alpha}I_n & -I_n & 0_n & 0_n \\ 0_n & s^{\alpha}I_n & -I_n & 0_n \\ 0_n & 0_n & s^{\alpha}I_n & -I_n \\ -A & 0_n & A_1 & s^{\alpha}E \end{bmatrix} \rightarrow \begin{bmatrix} 0_n & -I_n & 0_n & 0_n \\ s^{2\alpha}I_n & 0_n & -I_n & 0_n \\ 0_n & s^{2\alpha}I_n & 0_n & -I_n \\ -A & s^{\alpha}A_1 & A_1+s^{2\alpha}E & s^{\alpha}E \end{bmatrix}$$

$$\rightarrow \begin{bmatrix} 0_n & -I_n & 0_n & 0_n \\ 0_n & 0_n & -I_n & 0_n \\ 0_n & 0_n & 0_n & -I_n \\ -A+s^{2\alpha}A_1+s^{4\alpha}E & s^{\alpha}A_1+s^{2\alpha}E & A_1+s^{2\alpha}E & s^{\alpha}E \end{bmatrix}$$

$$\rightarrow \begin{bmatrix} 0_n & -I_n & 0_n & 0_n \\ 0_n & 0_n & -I_n & 0_n \\ 0_n & 0_n & 0_n & -I_n \\ -A+s^{2\alpha}A_1+s^{4\alpha}E & 0_n & 0_n & 0_n \end{bmatrix}$$

Hence

$$\det(s^{\alpha}\tilde{E}-\tilde{A})=\det(s^{4\alpha}E+s^{2\alpha}A_1-A). \tag{15}$$

This completes the proof for $k_2=4$ and $k_1=2$. Proof for other values of k_2 and k_1 is similar.

From Lemma 1 it follows that if (3) holds then the system (1) is regular.

From the theory of stability of linear fractional order systems given by Matignon [19] (see also [3, 22, 23] we have the following.

Lemma 2. The equivalent fractional order system (9) with non-singular matrix $\tilde{E}$ (for simplicity we assume $\tilde{E}=I_{k_2n}$), of the form

$$D_t^{\alpha}\tilde{x}(t)=\tilde{A}\tilde{x}(t), \tag{16}$$

is stable if and only if the fractional degree characteristic polynomial

$$w(s)=\det(s^{\alpha}I_{k_2n}-\tilde{A}) \tag{17}$$

has no zeros in the closed right-half of the Riemann complex surface, i.e.

$$w(s)\neq 0 \ \text{ for } \ \operatorname{Re} s\geq 0, \tag{18}$$

or equivalently, the following condition is satisfied

$$|\arg\lambda_i(\tilde{A})| > \alpha\frac{\pi}{2}, \quad i = 1,2,...,n, \tag{19}$$

where $\lambda_i(A)$ is the i-th eigenvalues of matrix $\tilde{A}$.

The stability region of the system (16), described by (19), is shown in Fig. 1.

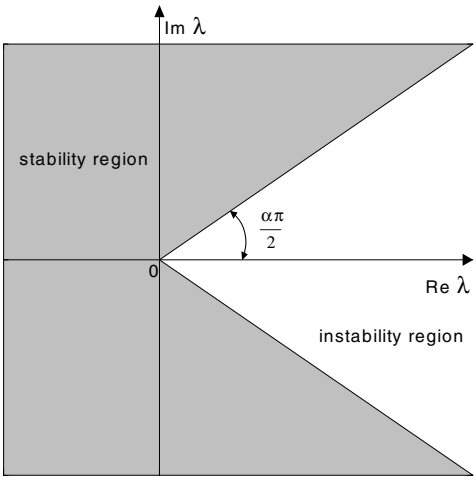

Fig. 1. Stability region of the fractional system (16) in the λ-plane

The condition (19) can be rewritten in the form [3]

$$\gamma > \alpha\frac{\pi}{2}, \text{ where } \gamma = \min_i |\arg\lambda_i(\tilde{A})|. \tag{20}$$

From the theory of stability of linear descriptor systems we have the following lemma [10].

Lemma 3. The equivalent descriptor regular system (9) with $\alpha = 1$, of the form

$$\tilde{E}\dot{\tilde{x}}(t) = \tilde{A}\tilde{x}(t), \tag{21}$$

is stable if and only if

$$\sigma(\tilde{E},\tilde{A}) \subset \boldsymbol{C}^- = \{\lambda : \lambda \in \boldsymbol{C}, \operatorname{Re}\lambda < 0\}, \tag{22}$$

where

$$\sigma(\tilde{E},\tilde{A}) = \{\lambda : \lambda \in \boldsymbol{C}, \lambda \text{ is finite}, \det(\lambda\tilde{E} - \tilde{A}) = 0\} \tag{23}$$

is the set of finite poles of the system containing at most $\tilde{n}_e$ (12) complex numbers.

The finite poles of (21) are the finite eigenvalues of the matrix pair $(\tilde{E}, \tilde{A})$. These eigenvalues can be computed by using the command $\text{eig}(\tilde{A}, \tilde{E})$ of the MATLAB.

From Lemmas 1 and 2 we have the following theorem.

Theorem 1. The two-term descriptor regular system of fractional orders described by the state equation (1) is stable if and only if all finite roots λ_i of the natural degree characteristic equation

$$\det H(\lambda) = \det(\lambda^{k_2} E + \lambda^{k_1} A_1 - A) = 0, \tag{24}$$

or equivalently, all finite eigenvalues λ_i of the pair of matrices $(\tilde{E}, \tilde{A})$, of the form given in (10), satisfy the condition

$$|\arg \lambda_i| > \alpha \frac{\pi}{2}, \tag{25}$$

i.e. lie in the stability region shown in Fig. 1.

Proof. Stability of the fractional descriptor two-term regular system (1) if equivalent to stability of the associated fractional descriptor system (9) with commensurate orders. Stability of this system depends from its finite poles which are finite eigenvalues of pair of matrices $(\tilde{E}, \tilde{A})$. Finite eigenvalues of $(\tilde{E}, \tilde{A})$ and finite roots of (24) are the same. Therefore, according to Lemma 3, these roots (eigenvalues) must be located in stability region shown in Fig. 1. This completes the proof.

Note that the equation (24) is obtained by substitution $s^{\alpha} = \lambda$ in the characteristic polynomial (13).

From the form (10) of matrix $\tilde{E}$ and (12) it follows that the set of finite roots of (24) (finite eigenvalues of pair $(\tilde{E}, \tilde{A})$) contains at most

$$N = (k_2 - 1)n + n_e < k_2 n \tag{26}$$

complex numbers, where $n_e = \text{rank } E < n$.

From Theorem 1 we have the following lemmas.

Lemma 4. The two-term descriptor regular system (1) is stable if and only if

$$\alpha < \frac{2\gamma}{\pi}, \quad \gamma = \min_i |\arg \lambda_i|, \tag{27}$$

where λ_i are the finite roots of the characteristic equation (24) (finite eigenvalues of pair $(\tilde{E}, \tilde{A})$).

Lemma 5. If all finite roots λ_i of the characteristic equation (24) (finite eigenvalues of pair $(\tilde{E}, \tilde{A})$) have negative real parts, then the fractional descriptor two-term regular system (1) is stable for all $\alpha \in (0, 1]$.

The method of Theorem 1 requires computation of eigenvalues of pair $(\tilde{E}, \tilde{A})$. Size of these matrices may be very high. If, for example, $\alpha_2 = 0.97$ and $\alpha_1 = 0.7$ in (7), then in (1) we have $\alpha = 0.01$, $k_2 = 97$ and $k_1 = 70$. In this case size of the matrices (10) is $97n \times 97n$. Hence, the investigation of stability of the fractional system (1) by checking the condition of Theorem 1 or the condition (27) can be inconvenient.

Therefore, we apply the frequency domain method to stability checking of the descriptor fractional system (1). This method has been proposed in [1] for asymptotic stability analysis of fractional order continuous-time linear systems described by the transfer function and in [3, 4] for the systems described by state space models. Results of these papers are described in [15, Chapter 9].

Denote by δ the fractional degree of the characteristic polynomial (13). It is easy to see that $\delta \leq N\alpha$, where N is defined by (26).

Let $w_r(s)$ be the reference stable fractional polynomial of degree δ. This polynomial can be chosen in the form

$$w_r(s) = (s + c)^{\delta}, \quad c > 0. \tag{28}$$

Let us consider the rational function

$$\psi(s) = \frac{w(s)}{w_r(s)} = \frac{\det H(s)}{w_r(s)}, \tag{29}$$

where $\det H(s)$ is defined in (13).

Theorem 2. The fractional order system (1) is stable if and only if

$$\underset{\omega \in (-\infty, \infty)}{\Delta \arg} \ \psi(j\omega) = 0, \tag{30}$$

where $\psi(j\omega) = \psi(s)$ for $s = j\omega$ and $\psi(s)$ is defined by (29).

Proof. From (29) it follows that

$$\underset{\omega \in (-\infty, \infty)}{\Delta \arg} \ \psi(j\omega) = \underset{\omega \in (-\infty, \infty)}{\Delta \arg} \ w(j\omega) - \underset{\omega \in (-\infty, \infty)}{\Delta \arg} \ w_r(j\omega). \tag{31}$$

From the Argument Principle it follows that the fractional degree characteristic polynomial (13) is stable if and only if

$$\underset{\omega \in (-\infty, \infty)}{\Delta \arg} \ w(j\omega) = \underset{\omega \in (-\infty, \infty)}{\Delta \arg} \ w_r(j\omega) = \delta\pi. \tag{32}$$

From (31) it follows that (32) holds if and only if (30) is satisfied.

Satisfaction of (30) means that plot of the function $\psi(j\omega)$ does not encircle or cross the origin of the complex plane as ω runs from $-\infty$ to ∞.

From (29) and (13) it follow that if the reference polynomial has the form (28) then

$$\psi(0) = \det(-A)/c^{\delta} \tag{33}$$

and

$$\psi(\infty) = \lim_{\omega \to \pm\infty} \frac{\det((j\omega)^{k_2\alpha} E + (j\omega)^{k_1\alpha} A_1 - A)}{(j\omega + c)^{\delta}}. \tag{34}$$

From (33) it follows that $\psi(0) \le 0$ if $\det(-A) \le 0$. Hence, from Theorem 2 we have that the fractional order system (1) is not stable if $\det(-A) \le 0$ and $\psi(\infty) \ge 0$.

4 Illustrative Example

Example 1. Consider the system (1) with $n = 3,\ k_2 = 2,\ k_1 = 1$ and the matrices

$$E = \begin{bmatrix} 1 & 1 & 0 \\ 0 & 1 & 0 \\ 0 & 0 & 0 \end{bmatrix},\ A_1 = \begin{bmatrix} -0.5 & -0.2 & 0 \\ -0.4 & 0.1 & -0.3 \\ 0 & -0.3 & 0.1 \end{bmatrix},\ A = \begin{bmatrix} -0.8 & -0.1 & 0.2 \\ 0.6 & -3.7 & 0.7 \\ 0.1 & 0.8 & -3.3 \end{bmatrix}. \tag{35}$$

Find values of fractional order α for which the system is stable.

From (10) it follows that the matrices of equivalent single-term fractional system (9) are as follows

$$\tilde{E} = \begin{bmatrix} I_3 & 0_3 \\ 0_3 & E \end{bmatrix} \in R^{6\times 6},\ \tilde{A} = \begin{bmatrix} 0_3 & I_3 \\ A & -A_1 \end{bmatrix} \in R^{6\times 6}. \tag{36}$$

Using the command $\text{eig}(\tilde{A}, \tilde{E})$ of the MATLAB we compute the finite eigenvalues of $(\tilde{E}, \tilde{A})$: $\lambda_1 = -32.2116;\ \lambda_{2,3} = -0.1845 \pm j2.1154;\ \lambda_{4,5} = 0.2427 \pm \text{j}0.7649.$

From (27) we have

$$\gamma = \min_i |\arg \lambda_i| = \arctan(0.7649/0.2427) = 1.2635 \tag{37}$$

and

$$\alpha < 2\gamma/\pi = 0.8044. \tag{38}$$

Hence, according to Lemma 4, the system is stable for $0 < \alpha < 0.8044$.

Now we apply the frequency domain method given in Theorem 2.

From (35), (36) it follows that the characteristic polynomial (13) of the system has the fractional degree $\delta = N\alpha = 5\alpha$, since, according to (26), $N = (k_2 - 1)n + n_e = 5$.

Plot of the function

$$\psi(j\omega) = \frac{\det H(j\omega)}{(j\omega + 4)^{5\alpha}},\ \ \omega \in (-\infty, \infty), \tag{39}$$

is shown in Fig. 2 for $\alpha = 0.75$ and $\alpha = 0.85$.

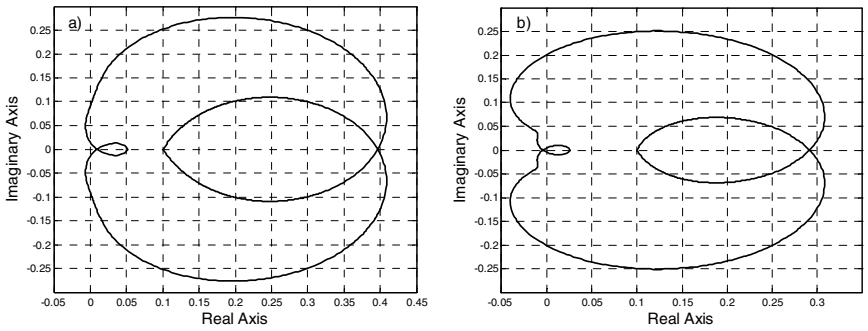

Fig. 2. Plot of the function (39): a) for α=0.75: b) for α=0.85

From (33), (34) and structure of the matrix $H(s) = s^{2\alpha}E + s^{\alpha}A_1 - A$ it follows that $\psi(0) = 0.0517$ for $\alpha = 0.75$ and $\psi(0) = 0.0258$ for $\alpha = 0.85$. Moreover, $\lim_{s\to\infty} \det H(s) = 0.1$, which means that $\psi(\infty) = 0.1$ for $\alpha = 0.75$ and $\alpha = 0.85$.

From Fig. 2 it follows that plot of (39) does not encircle the origin of the complex plane for $\alpha = 0.75$ and encircles for $\alpha = 0.85$. This means, according to Theorem 2, that the system (1), (35) is stable for $\alpha = 0.75$ and unstable for $\alpha = 0.85$.

5 Concluding Remarks

The stability problem of continuous-time descriptor two-term linear system (1) with commensurate orders of fractional derivatives has been considered.

It has been shown that stability of the system is equivalent to satisfaction of the condition (25) for all finite roots of the natural degree characteristic equation (24). These roots are the finite eigenvalues of the pair of matrices $(\tilde{E}, \tilde{A})$ of the form (10) (Theorem 1).

The frequency domain method for stability checking of the system is given in Theorem 2. This method is simpler to apply in the case of large values of k_2.

Acknowledgement. The work was supported by the National Science Center in Poland under grant N N514 638940.

References

1. Busłowicz, M.: Stability of Linear Continuous-time Fractional Order Systems with Delays of the Retarded type. Bull. Pol. Acad. Sci., Tech. Sci. 56, 319–324 (2008)
2. Busłowicz, M.: Robust Stability of Positive Discrete-time Linear Systems of Fractional Order. Bull. Pol. Acad. Sci., Tech. Sci. 58, 567–572 (2010)
3. Busłowicz, M.: Stability of State-Space Models of Linear Continuous-time Fractional Order Systems. Acta Mechanica et Automatica 5, 15–22 (2011)

4. Busłowicz, M.: Stability Analysis of Continuous-time Linear Systems Consisting of *n* Subsystems with Different Fractional Orders. Bull. Pol. Acad. Sci., Tech. Sci. 60, 279–284 (2012)
5. Busłowicz, M.: Simple Analytic Conditions for Stability of Fractional Discrete-time Linear Systems with Diagonal State Matrix. Bull. Pol. Ac.: Tech. 60(4), 809–814 (2012)
6. Busłowicz, M.: Frequency Domain Method for Stability Analysis of Linear Continuous-Time State-Space Systems with Double Fractional Orders. In: Mitkowski, W., Kacprzyk, J., Baranowski, J. (eds.) Theory & Appl. of Non-integer Order Syst. LNEE, vol. 257, pp. 31–39. Springer, Heidelberg (2013)
7. Busłowicz, M., Kaczorek, T.: Simple Conditions for Practical Stability of Linear Positive Fractional Discrete-time Linear Systems. Int. J. Appl. Math. Comput. Sci. 19(2), 263–269 (2009)
8. Busłowicz, M., Ruszewski, A.: Necessary and Sufficient Conditions for Stability of Fractional Discrete-time Linear State-space Systems. Bull. Pol. Acad. Sci., Tech. Sci. 61 (2013) (in print)
9. Diethelm, K.: The Analysis of Fractional Differential Equations. LNM. Springer, Heidelberg (2010)
10. Duan, G.-R.: Analysis and Design of Descriptor Systems. AMM, vol. 23. Springer, New York (2010)
11. Duan, G.-R., Huang, L.: Robust Pole Assignment in Descriptor Second-order Dynamical Systems. Acta Automatica Sinica 33(8), 888–892 (2007)
12. Dzieliński, A., Sierociuk, D.: Stability of Discrete Fractional State-Space Systems. Journal of Vibration and Control 14, 1543–1556 (2008)
13. Jiao, Z., Chen, Y.-Q.: Stability Analysis of Fractional-Order Systems with Double Noncommensurate Orders for Matrix Case. Fractional Calculus Applied Analysis, An Int. J. for Theory and Applications 14, 436–453 (2011)
14. Kaczorek, T.: Necessary and Sufficient Stability Conditions of Fractional Positive Continuous-time Linear Systems. Acta Mechanica et Automatica 5, 52–54 (2011)
15. Kaczorek, T.: Selected Problems of Fractional Systems Theory. LNCIS, vol. 411. Springer, Heidelberg (2011)
16. Kaczorek, T.: Stability of Descriptor Positive Linear Systems. COMPEL 32(1), 412–423 (2013)
17. Kaczorek, T.: Descriptor Fractional Linear Systems with Regular Pencils. Asian J. Control 15(4), 1–14 (2013)
18. Kilbas, A.A., Srivastava, H.M., Trujillo, J.J.: Theory and Applications of Fractional Differential Equations. Elsevier, Amsterdam (2006)
19. Matignon, D.: Stability Result on Fractional Differential Equations with Applications to Control Processing. In: IMACS-SMC2, Lille, France, pp. 963–968 (1996)
20. Monje, C., Chen, Y., Vinagre, B., Xue, D., Feliu, V.: Fractional-Order Systems and Controls. Springer, London (2010)
21. Podlubny, I.: Fractional Differential Equations. Academic Press, San Diego (1999)
22. Sabatier, J., Moze, M., Farges, C.: LMI Stability Conditions for Fractional Order Systems. Computers and Mathematics with Applications 59, 1594–1609 (2010)
23. Tavazoei, M.S., Haeri, M.: Note on the Stability of Fractional Order Systems. Mathematics and Computers in Simulation 79, 1566–1576 (2009)

Design of Integrated Information Systems for the Security of People and Objects

Małgorzata Cupriak[1], Sławomir Jasiński[1], and Małgorzata Kaliczyńska[2]

[1] Kontron East Europe sp. z o.o., Warsaw, Poland
{slawomir.jasinski,malgorzata.cupriak}@kontron.pl
[2] Industrial Research Institute for Automation and Measurements PIAP, Warsaw, Poland
mkaliczynska@piap.pl

Abstract. The article presents a number of issues concerning the integration of many information systems and automation equipment in order to ensure full control and improve the user experience. Particular attention is paid to the safety systems installed in public utility facilities, including fire protection systems used in urban subways objects (with Warsaw metro as an example). Structure of the integrating system is described and an overview is made of the specialised components used in its design and implementation. Requirements are also presented for obtaining technical approval. Experience gained during the design, implementation and testing of the integrated security system is also summarized.

Keywords: safety system, IT system, detection, object, integration.

1 Introduction

Modern objects of common use, such as factories, shopping malls, airports, train stations, subways are equipped with numerous electronic systems used to ensure automatic control of their proper operation, as well as security of facilities and their users. Often these systems come from different manufacturers, operate independently with various functionalities, installed with the introduction of new technologies. Multiplying systems from different manufacturers, as well as the irresponsible behaviour of users, (often bystanders than service staff) can be a source of unexpected behaviour of individual system components, including unauthorized alarms. In such a situation, the additional master control is required, allowing the supervision carried out by the operator and rapid response, such as switching off the alarms activated accidentally.

2 Overview of Common Solutions

There are several solutions of systems integrating security systems. Some of them are of the general purpose; others are dedicated for operation in particular facilities. Most often used on the domestic market are GEMOS and DMS8000 systems.

R. Szewczyk, C. Zieliński, and M. Kaliczyńska (eds.), *Recent Advances in Automation, Robotics and Measuring Techniques*, Advances in Intelligent Systems and Computing 267,
DOI: 10.1007/978-3-319-05353-0_6,

GEMOS Facility Management System [1] integrates all safety and automation systems in the building, improving safety standard level of the facility, with the simultaneous reduction of its operating costs. It serves as a master control panel, which collects and logs alarms and other information from safety systems and technical supervision devices, to provide a uniform and consistent information with all the necessary instructions including the actions taken.

The DMS8000 integrating device [2] implements interaction of the building fire protection systems, being used in small objects using a small number of control panels. It can be configured in the point-to-point architecture, providing the redundant connection.

One of the major risks that can disrupt the safe operation of public facilities is fire. It is accompanied by panic, chaos, threatens people with carbon monoxide poisoning, burns, or even death. Therefore, this aspect is particularly seriously analysed, and safety ensuring devices are required.

At most stations of the Warsaw metro, the fire protection system is used supported by the EBL G3 microprocessor control panel designed to work with the analogue addressable smoke detectors, conventional thermal detectors, manual fire alarms, control modules, as well as with the acoustic and optical signalling devices. Each control panel makes it possible to connect up to 4 loops with sensors and signalling devices. The control panels may be connected to form a network of up to 30 control panels, which enlarges the system capacity to more than 15,000 of fire points. The control panels communicate using the doubly terminated bus TLON network (connection redundancy). Each of the control panels has access to all information from other control panels in the same network – the control panels are peer-to-peer. One may monitor system state from any location with Internet access.

3 PEP110 Integrating System – Architecture

Analysis of the functionality and features of the existing solutions contributed to the decision to design the PEP110 integrating system, which will make connection and cooperation possible of various systems, providing a uniform service platform. These may be systems that are used in railway traffic control [5, 6], and above all guarantee safety:

- fire protection system,
- detection system for objects in the track (people and items),
- intrusion prevention system [4],
- traffic situation monitoring system,
- operation diagnostics system for individual system components and equipment,
- traveller information system,
- audible warning system,
- communication systems,
- automation systems,

and/or other required systems.

The integrating system should allow (based on messages, dynamic graphics and activity results of the diagnostic functions) forwarding supervision services necessary information to support decision-making in the state of crisis in the facility. The integrating system should be an open, scalable software-hardware platform, fully independent from the manufacturers of the integrated systems and equipment. It should allow full interoperability of various systems, their easy setup and maintenance. The facility layouts should be presented graphically. The integrating system should not only monitor, visualize, and archive data, it should also permit manual control override of devices and integrated systems, control with the highest priority in relation to automatic control, which is implemented by the fire protection control panel and its I/O modules installed on the loop detection circuits. The system should integrate the various subsystems using open communication standards (CAN, Profibus, Ethernet, LON, etc.), popular network protocols and reliable transmission media.

It should be possible to build a complex management system for the technical equipment of the facility (Fig. 1) containing maximum 120 local and remote monitoring centres.

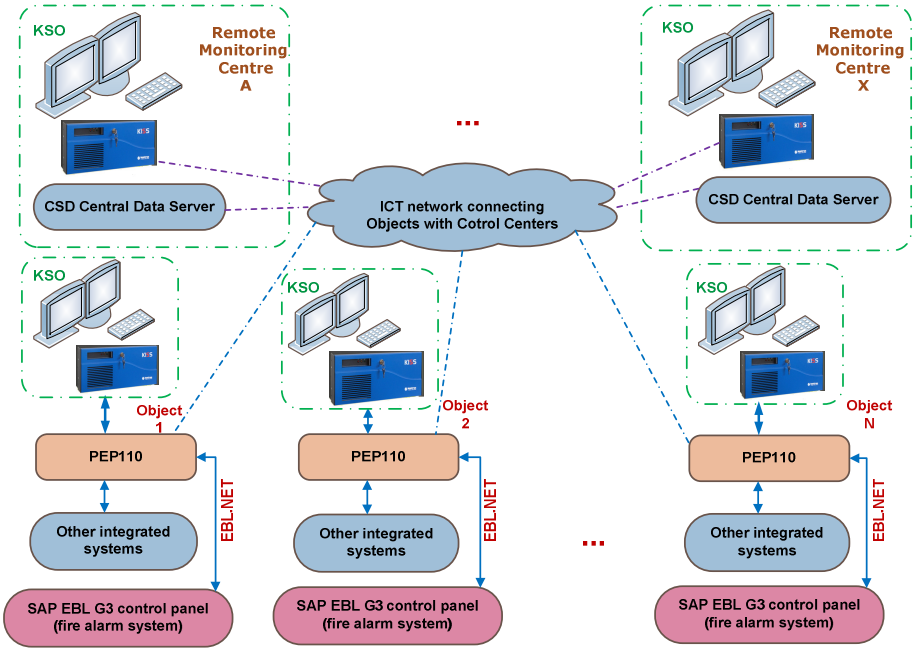

Fig. 1. Functional diagram of the complex management system for the technical equipment of the facility

3.1 Operator's Console

Console (terminal) of the integrating system should be realized in the form of the KSO monitoring and imaging stand. Depending on needs and arrangements with the recipient, the integrating system can be supported by many KSO stands. Every KSO

console is a computer workstation with two monitors. The KSO console software should allow data acquisition, imaging, and supervisory control.

The PEP110 integrating system consists of the following devices:

- PEP110-M – hardware module provided with the IT platform (Fig. 2), housed in the control cabinet. The PEP110-M consists of modular drivers for the following purpose:
  - KS – control computer for technical devices not connected directly with fire protection devices;
  - KWDx – data exchange computer ensuring two-way communication with the SAP EBL G3 system control panel (based on Ethernet technology); installed software (using components of the EBL.NET library) enables the overarching scenarios and manual control. To ensure redundancy of a connection with the EBL G3 control panel, the PEP110-M uses at least two KWDx modules (x stands for the next KWD computer.)
- KSO – console (terminal) for the PEP100 integrating system is the monitoring and imaging stand. Depending on needs, PEP100 can be supported by many KSO stands. Every KSO console is a computer workstation with two LCD monitors. Its software allows data acquisition, imaging, and supervisory control.
- KD20 – local diagnostic KD20 computer, designed to record data (events and states of the system) and for diagnostics, ensures transmission access to the facility signals.

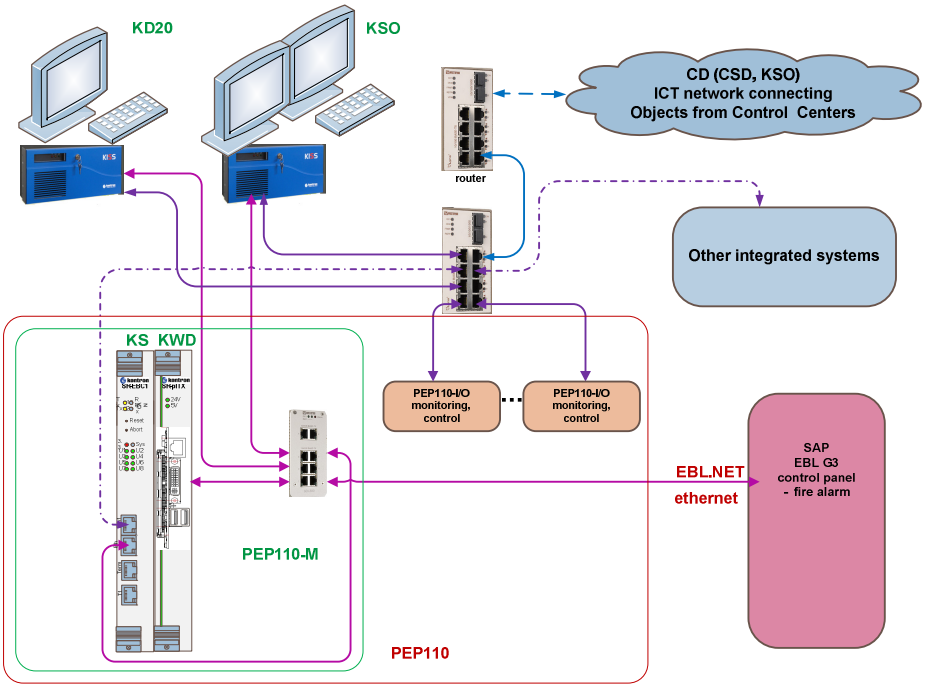

Fig. 2. Functional diagram of the integrating system

Software requirements of the KSO control desk:

a) operating system – Windows XP Embedded or newer,
b) the system should allow for the collection of information on alerts, notifications and actual parameters transferred from the connected control units and controls for fire protection equipment and display them in a transparent manner on one or more KSOs,
c) system use (operation) should be implemented using standard peripherals (mouse, touchpad, keyboard),
d) the system should be adapted to display information on multiple monitors, one of them, selected from the connected monitors, should display the fire information only,
e) all events taking place throughout the system should be automatically recorded in real time; a function is required to print this information on request, also including the use of appropriate filters,
f) information about failures signalled in the connected control panels of the fire protection system should also be indicated visually and acoustically by the KSO,
g) information about any disruption of data transmission should be signalled visually and acoustically by the KSO,
h) disruptions of EBL G3 operation should not affect the operation of the integrating system, disruptions of KSO operation should not affect the work of EBL G3,
i) imaging system should enable easy discovery of the detector element based on designations consistent with those used when handling EBL G3 and display of the current status of the element, with automatic indication of its location on the layout,
j) in the absence of communication between the facility device and fire alarm system., information about such a situation should be indicated in the computer system; the notification time depends on the delays characteristic of the signalling system communication protocol and must not exceed 300 seconds after the connection is interrupted,
k) all messages received by the KSO should be confirmed after their safe recording by the recorder; the messages may not be processed before they are secured,
l) new alarm message should be displayed until it is confirmed by the stand staff member or another authorized person,
m) damage messages should be processed in the same way as alarm messages.
n) messages should be retrieved from the message queue in the order they are received,
o) the system should allow the on-demand presentation of messages sent from each EBL G3 control panel connected to the system,
p) the system should provide in real time all unapproved fire alarm messages,
q) the system should allow for the acceptance of messages; the message signalisation ends with the acceptance of the presented warning indication,

r) damage messages should include specific data, at least: the type of damage (eg power failure), the event (loss of primary power supply), the date and time of the event,
s) event registration should be implemented in at least two registers (redundant write), located in the KD20 diagnostic computers on the stands and in an additional CSD central data server in the Control Centre,
t) registry damage (bad sectors, lost messages) should be detected by the system,
u) all messages received by the KSO should be recorded with the date and time of confirmation (with an accuracy of 1 s),
v) all information about damage and local information generated by the KSO should be recorded with the date and time of generation,
w) capacity of the memory used should guarantee a long-term recording (1–2 years),
x) register shall enable the preservation of data (messages and local information) in the event of a total loss of power,
y) in the case of a corrupted registry warning alarm should be generated within 10 seconds of receiving a message by the KSO that could not be registered because of a corrupted registry.

3.2 Imaging the Status of all Integrated Systems

The system presents graphical information about the status of all monitored/ integrated systems and their constituent components (individual inputs, outputs, sensors, zones, collective sensors informing about the states, etc.). Imaging system takes into account the states reported by the device:

- normal,
- damage,
- alarm/excitation.

The presentation of states of each component is implemented in a manner agreed upon with the customer.

3.3 Functional Requirements for the KD20 Diagnostic Computer

KD20 diagnostic computers should allow for:

- registration of data (events and states of the system) in three independent registers; lack of registration should be signalled to the system operator,
- diagnostics of the hardware, system, software, communication with other systems,
- transmission access to facility signals,
- supervision of the system, as well as processing and analysis of all the information from the facility – from field devices and SAP Control Panel.